

# Response of Export Production and Dissolved Oxygen Concentration in Oxygen Minimum Zones to pCO<sub>2</sub> and Temperature Stabilization Scenarios in the Biogeochemical Model HAMOCC 2.0

Authors: T. Beaty, A.M.E. Winguth, T. Hughlett, C. Heinze

## **Modification to the manuscript:**

In the substantially revised version, we have added an analysis of seven new simulations in order to address the Editors and Reviewers concerns. Four simulations address how the simulated DO concentrations respond to changes in ventilation in the model. Three additional simulations were added to address changes in solubility by holding POC production at preindustrial levels while increasing CO<sub>2</sub> and seawater temperature. Each of the simulation were discussed and integrated into the manuscript. Addition figures were added as needed to fully discuss these simulations. Second, dissolved organic carbon is considered in the new analysis giving further insight into the changes in DO concentration in the HAMOCC model. Furthermore, the revised manuscript focuses more on long-term changes in the OMZ. The HAMOCC model is beneficial to investigate long-term biogeochemical cycles that cannot explored by fully couple climate models due to the high computational expenses of these models. Thus, we hope that we have better conveyed the purpose and validity of the work.

## List of Changes to the manuscript

- 4 new ventilation simulations
- 3 additional solubility simulation
- The addition of the role of DOC to the discussion, figures and table
- Addition figures to support the text both within the manuscript and as supplementary data

## **Point by point comments for Referee #1:**

General assessment; we appreciate the referee's comments and suggestions. We agree with the referee that consideration of changes in ventilation is of importance also for the distribution of dissolved oxygen and the distribution of OMZs in the oceans. However, we originally did not aim to consider ventilation changes and to focus on temperature induced changes only. The reason for this was that oxygen and radiocarbon are not very well correlated in the ocean water column and ventilation changes may mask the temperature effect. Furthermore, HAMOCC is a biogeochemical model designed to long integration with low computational cost to allow adjustment with sediment geochemistry in the timescale of 10,000 yrs or more. In contrast, comprehensive Earth System Models can run only in a order of several 1,000 yrs. This study focuses on the long-term trend of the oxygen minimum zone by the changes in the biological and solubility pump in response to global temperature on a longer time sales. Interactive changes between ocean ventilation and carbon cycle on the millennial time scale with a similar model has been published elsewhere (e.g. in Mikolajewic et al. 2007, *Climate Dynamics*, or Winguth et al., 2005 *JGR*). We have, however, included an experiment on the effect of a change in ocean ventilation in our revision. Additionally a sensitivity experiment was simulated where the ocean ventilation is shutdown, as an extreme scenario. This will provide insight into the maximum effect of potential ventilation changes on dissolved oxygen distribution in the biogeochemical model.

Page 1 line 18; Yes, we have clarify this sentence to include the distribution of CO<sub>2</sub> dissolution.

Page 2 lines 2 and 3; We have change the units of dissolved oxygen to  $\mu\text{mol kg}^{-1}$  throughout the manuscript.

Page 2 line 3; Sentence has been corrected accordingly.

Page 2 line 18; We have add a plots, results and discussions on the response DOC in the model.

Page 2 lines 23-26; This is an offline model and flow fields are an input into the model. Therefore we focus on the long term response of DO to changes in POC export production and changes in oxygen solubility in this study.

Page 4 lines 26-28; We have add plots, results and discussions on the response DOC in the model.

Page 5 lines 16-19; To clarify the sensitivity study, we applied a global uniform temperature change in the ocean in each simulation.

Page 6 lines 7-9; See major comments. Global mean temperature anomalies have been applied.

Pages 8-12 Supplementary figures have been added to support the manuscript.

Page 12 lines 16-18; The sentence has be corrected to state that Dissolved oxygen increases to  $>300 \mu\text{mol L}^{-1}$  in the deep-sea and  $>200 \mu\text{mol L}^{-1}$  in the intermediate water masses.

Page 12 lines 29-30; the purpose of this study is to analyze the strength of the following two OMZ controls: changes in the solubility and biological pump.

Page 13 first paragraph. A figure for dissolved organic carbon in conjunction with particulate organic carbon was added to the supplementary data.

Table 1; The 's' in  $s\text{CO}_2$  will be removed from the table. The 's' is an indicator meaning within the water column in the model and is not necessary in the table.

Figure 2, 5, 7, 8 Many figures have changed in this revision but all corrections were applied if applicable

## Point by point comments for Referee #2:

### General comments

Thank you for your comments and suggestions. I agree that ventilation is an important variable for determining changes in OMZs (see also our respective response to reviewer #1). Though we aimed at focusing on the temperature and  $\text{CO}_2$  effects on the ocean oxygen distribution, we have added respective experiments on ocean circulation changes (see also our response to reviewer #1). We focus on changes in the biological pump and how these changes affect ocean interior oxygen and OMZs. We have provided a better separation of the solubility and biological productivity effects in additional experiments were POC remains constant and  $p\text{CO}_2$  is increased. The model does overestimate productivity at the equator due to nutrient trapping (see Najjar et al., 1992, GBC). Productivity is temperature dependent; however, remineralization is dependent on a fixed Redfield ratio and oxygen consumption (i.e. POC concentration). A plot of  $\text{PO}_4$  has been added to the supplementary data for clarification.

### Specific comments

1. We have revisited the text to make sure figures are referenced correctly.
2. Either by merging or separating many sections changed in the manuscript. Also, comparisons to observed data has been added to the supplementary data.
3. This sentence will be corrected to state that the bottom boundary of the OMZ does not deepen.
4. Figure 4 illustrates the changes to the dissolved oxygen profile through the core of the OMZ for each simulation as well as observed data. Illustrating the profile this way allows the reader to evaluate the depth of the oxycline. Unfortunately, this same detail cannot be accomplish with the plotting program that accompanies HAMOCC.
5. The atmospheric oxygen simulation has been removed from the manuscript.

6. All experiments including the reduced biology scenario are run from a near-steady state condition and integrated for 30,000yrs with the exception of the new ventilation simulations and steady POC. These simulations were reduced to 10,000 years since max DO loss occurs ~ 2000 years after max pCO<sub>2</sub> is reached. CO<sub>2</sub> and O<sub>2</sub> are actively exchanged between the ocean and the atmosphere.
7. This statement has been removed from the manuscript. Nonetheless, to clarify strong upwelling in the tropical Pacific Ocean could transport high-nutrient and oxygen depleted water masses to the surface; however, in the model these waters are at equilibrium with the atmospheric and therefore the effect of the upwelling on DO concentrations is diminished in the model.
8. The model assumes a constant Redfield ratio following Maier-Reimer, 1993, GBC. However, potential changes in the Redfield ratio due to ecosystem dynamics could result in changes in POC and thus the OMZ (e.g. as resulting in a mesocosm experiment, see Riebesell et al., 2007, Nature).
9. Variables and units have been added to the color bar.

1 **Response of Export Production and Dissolved Oxygen**  
2 **Concentrations in Oxygen Minimum Zones to pCO<sub>2</sub> and**  
3 **Temperature Stabilization Scenarios in the Biogeochemical**  
4 **Model HAMOCC 2.0**

5  
6 **T. Beaty<sup>1</sup>, C. Heinze<sup>2,3</sup>, T. Hughlett<sup>4</sup>, and A. M. E. Winguth<sup>2</sup>Winguth<sup>4</sup>, and C.**  
7 **Heinze<sup>3,4</sup>**

Formatted: Superscript

Formatted: Superscript

8 [1]{New Mexico Consortium-Biological Laboratory, Los Alamos, New Mexico}

9 ~~[2]{Department of Earth and Environmental Sciences, University of Texas at Arlington,~~  
10 ~~Arlington, Texas}~~

11 ~~[23]~~{Geophysical Institute, University of Bergen, and Bjerknes Centre for Climate Research,  
12 Bergen, Norway}

13 ~~[34]~~{Uni Research Climate, Bergen, Norway}

14 ~~[42]~~{Department of Earth and Environmental Sciences, University of Texas at Arlington,  
15 Arlington, Texas}

16  
17 Correspondence to: T. Beaty (tbeaty@newmexicoconsortium.org)

18  
19 **Abstract**

20 Dissolved oxygen (DO) concentration in the ocean is an important component of marine  
21 biogeochemical cycles and will be greatly altered as climate change persists. In this study a  
22 global oceanic carbon cycle model (HAMOCC 2.0) is used to address how mechanisms of  
23 oxygen minimum zones (OMZ) expansion respond to changes in CO<sub>2</sub> radiative forcing.  
24 Atmospheric pCO<sub>2</sub> is increased at a rate of 1% annually and the model is stabilized at 2 X, 4  
25 X, 6 X, and 8 X preindustrial pCO<sub>2</sub> levels. With an increase in CO<sub>2</sub> radiative forcing, the  
26 OMZ in the Pacific Ocean is controlled largely by changes in particulate organic carbon  
27 (POC) export, resulting in increased remineralization and thus expanding the oxygen  
28 minimum zones within the tropical Pacific Ocean. A potential decline in primary producers in

1 the future as a result of environmental stress due to ocean warming and acidification could  
2 lead to a substantial reduction of ~~POC export production, vertical POC flux, vertical carbon~~  
3 ~~flux~~ and thus increased DO concentration particularly in the Pacific Ocean at a depth of 600-  
4 800 m. In contrast, the vertical expansion of the OMZs within the Atlantic ~~and Indian Oceans~~  
5 ~~is~~are linked to ~~reduced oxygen solubility, increases POC flux, particulate organic carbon as well~~  
6 ~~as changes in oxygen solubility with increasing seawater temperature, due to rise in potential~~  
7 ~~temperature and to a lesser extent changes in remineralization rates.~~ Changes in oxygen  
8 ~~solubility, Total dissolved organic carbon and increase SST~~ also lead to the formation of a new  
9 OMZ in the western sub-tropical Pacific Ocean. The development of the new OMZ results in  
10 dissolved oxygen concentration of  $\leq 50 \mu\text{mol kg}^{-1}$  throughout the equatorial Pacific Ocean at  
11 ~~four~~<sup>4</sup> times preindustrial pCO<sub>2</sub>. ~~Total ocean area—volume~~ with dissolved oxygen  
12 concentrations of  $\leq 50 \mu\text{mol kg}^{-1}$  increases by 2.54%, 4.55.0%, and 7.610.5% for the 2 X, 4X,  
13 and 8 X CO<sub>2</sub> simulations, respectively.

Formatted: Superscript

Commented [TS1]: This statement has been changed from percent surface ocean area to percent change in total ocean volume as suggested by Review 1. I have either changed area to volume or included volume throughout the paper.

## 15 1 Introduction

16 Rapid increases in concentrations of greenhouse gases (CO<sub>2</sub>, CH<sub>4</sub>, and N<sub>2</sub>O) in the  
17 atmosphere since the 18<sup>th</sup> century have led to greenhouse gas radiative forcing and  
18 temperature change of 0.068 °C dec<sup>-1</sup> (Karl et al. 2015). Atmospheric CO<sub>2</sub> concentrations are  
19 predicted to continue to rise from the pre-industrial level of 280 ppmv up to ~800 ppmv by  
20 the year 2100 (IPCC 2013) or ~2000 ppmv by year 2400 under the assumption that all fossil  
21 fuel reservoirs are emitted into the atmosphere (Caldeira and Wickett 2003, Zachos et al.  
22 2008). The anthropogenic CO<sub>2</sub> will be partially sequestered by the ocean and by the biosphere  
23 on time scales on the order of 10<sup>4</sup> years. A ~~risen increase~~ in ~~ocean global~~ temperature  
24 ~~decreases the solubility of CO<sub>2</sub> in seawater and thus the tends to CO<sub>2</sub> uptake<sub>2</sub> in the~~  
25 ~~atmosphere into the ocean due to the decreased solubility of CO<sub>2</sub> in the ocean.~~ In addition, the  
26 ocean buffer capacity decreases with rising pCO<sub>2</sub>.

Formatted: Subscript

Formatted: English (United States)

27 Changes in climate as a result of CO<sub>2</sub> emission will affect the oxygen distribution in the  
28 ocean. DO (dissolved oxygen) concentration in the ocean is affected not only by ~~changes in~~  
29 ~~ocean ventilation solubility~~ but also by ~~solubility and~~ the biological pump (Volk and Hoffert  
30 1985). ~~The biological pump which~~ is controlled by export production, vertical carbon flux and  
31 decay of particulate organic carbon, ~~dissolved organic carbon~~ and by the transport of  
32 biogeochemical tracers by the ocean circulation. Variations in seasonal and long-term DO

1 concentration have been observed in sub-polar and subtropical regions (Whitney et al. 2007,  
2 Stramma et al. 2008). Climate models predict that DO concentrations in the ocean will  
3 continue to decline with the warming of the deep-sea due to the subsequent decline in  
4 solubility as well as variations in the biological pump due to changes in mixing and enhanced  
5 ocean stratification. The decrease of the DO concentration will likely result in the expansion  
6 of oxygen minimum zones (Sarmiento and Orr 1991, Sarmiento et al. 1998, Schmittner et al.  
7 2008, Shaffer et al. 2009) and a significant expansion of bottom water hypoxia ( $<10 \mu\text{mol O}_2$   
8  $\text{kg}^{-1}$ ).

9 There are five major non-seasonal OMZs discussed in the current literature, which are the  
10 eastern sub-tropical North Pacific OMZ ( $\sim 15^\circ\text{-}25^\circ\text{N}$ ), the eastern tropical Pacific OMZ  
11 (equatorial region), the eastern South Pacific OMZ ( $\sim 15^\circ\text{-}40^\circ\text{S}$ ), the Arabian Sea, the Bay of  
12 Bengal (Kamykowski and Zentara 1990, Karstensen et al. 2008, Paulmier et al. 2011), and  
13 one low oxygen zone (LOZ) or seasonal OMZ in the equatorial Atlantic. There is limited  
14 literature discussing the variability of the Atlantic and Indian Ocean OMZs; however, areas of  
15 the eastern North Atlantic OMZ are hypoxic with DO concentrations ranging from 40 to  $<2$   
16  $\mu\text{mol kg}^{-1}$  (Stramma et al. 2009, Karstensen et al. 2015). Pacific OMZs have been discussed  
17 extensively and there is strong evidence that expansion is already occurring (Oschlies et al.  
18 2008, Stramma et al. 2008, Keeling et al. 2010, Stramma et al. 2012). An expansion of the  
19 OMZ, a shoaling of the depth of hypoxia (DOH; shallowest depth at which OMZ criteria is  
20 met), or a shoaling of the OMZ cores into the photic zone could have severe impacts most  
21 notably the decline in ecosystems in the ocean.

22 In this study, the core of the OMZ is defined as a dissolved oxygen concentration of  $\leq 20$   
23  $\mu\text{mol kg}^{-1} \text{O}_2$  consistent with Helly and Levin 2004, Fuenzalida et al. 2009 and Paulmier et al.  
24 2011. The OMZ boundaries are described to have a DO concentration of  $50 \mu\text{mol kg}^{-1}$ . The  
25 maximum DO concentration of  $50 \mu\text{mol kg}^{-1}$  is more stringent than upper limits in other  
26 studies (Whitney et al. 2007, Karstensen et al. 2008); however, at these DO concentrations  
27 most microorganisms cannot survive (Kamykowski and Zentara 1990, Gray et al. 2002,  
28 Sarmiento and Gruber 2006, Paulmier et al. 2011) and therefore considered a reasonable  
29 criterion for non-seasonal OMZ. This study focuses on the extent of OMZ expansion and on  
30 determining the relative strengths of two mechanisms of OMZ expansion, the export  
31 production and oxygen solubility. the extent and physical properties of oxygen minimum

1 ~~zones expansion as well as the formation of new OMZs under future emission scenarios~~  
2 ~~including the mechanisms that lead to OMZ intensification.~~

## 4 **2 Model Description**

5 This study is conducted with the biogeochemical Hamburg Oceanic Carbon Cycle Model  
6 Version 2.0 (HAMOCC 2.0), which has been originally developed by Maier-Reimer and  
7 Hasselmann (1987) and Maier-Reimer (1993), and which has been expanded to include an  
8 iron cycle, sedimentary phosphorus cycle, and improved atmospheric dust parameterization  
9 (Palastanga et al. 2011, Palastanga et al. 2013). ~~HAMOCC was originally developed by~~  
10 ~~Maier Reimer and Hasselmann (1987) and Maier Reimer (1993). The annually averaged~~  
11 ~~version is computationally very economical and suitable for long term carbon cycle~~  
12 ~~simulations of several 10,000 years (Maier Reimer and Hasselmann, 1987, Heinze and Maier-~~  
13 ~~Reimer, 1999).~~ The model utilizes an E-grid (Arakawa and Lamb 1977) and has a horizontal  
14 resolution of  $\sim 3.5^\circ \times 3.5^\circ$  with grid points  $1.25^\circ$  north and south of the equator to resolve the  
15 equatorial upwelling belt. The model contains 11 layers (centered at 25,75,150, 250, 450, 700,  
16 1000, 2000, 3000, 4000, and 5000 meters) with a total depth of 5000 meters (Heinze et al.  
17 1999, Heinze et al. 2006, Heinze et al., 2009). HAMOCC 2.0 includes a sediment module  
18 with porewater and solid components that are coupled by a reaction rate. The sediment  
19 module includes one 10 cm thick layer of bioturbated sediment, which is further divided into  
20 11 sub-layers. A more detailed description of the sediment module can be found elsewhere  
21 (Heinze et al. 1991, Heinze et al. 1999, Heinze 2004).

22 The annually averaged version is computationally very economical and suitable for long-term  
23 carbon cycle simulations of several 10,000 years. Long-term integrations are possible with  
24 HAMOCC because of its coarse temporal and spatial resolution and because of the  
25 computationally efficient solution of tracer equations by an upstream formulation (Maier-Reimer  
26 and Hasselmann, 1987, Heinze and Maier-Reimer, 1999) that uses the prescribed annual  
27 average circulation and hydrography of the Large Scale Geostrophic (LSG) ocean general  
28 circulation model (Maier-Reimer et al., 1993; Winguth et al., 1999).

29 ~~Transport of tracers is simulated using present-day flow and hydrographic fields (Winguth et~~  
30 ~~al., 1999) from the Hamburg Large Scale Geostrophic (LSG) model (Maier-Reimer et al.~~  
31 ~~1993). The advection of tracers is iteratively solved by an upstream formulation (Maier-~~  
32 ~~Reimer and Heinze 1993).~~ Atmospheric CO<sub>2</sub> and O<sub>2</sub> are exchanged between the ocean surface

1 (top 50 m) and zonally mixed atmospheric boxes. The air-sea gas exchange of CO<sub>2</sub> is  
2 determined by the difference in the partial pressure of CO<sub>2</sub> in the sea surface and the  
3 atmospheric pCO<sub>2</sub>, the gas transfer velocity, and the requirement for a full equilibration of the  
4 surface layer inorganic carbon system. The gas exchange of oxygen is an order of magnitude  
5 faster than that of CO<sub>2</sub>. Oxygen exchange is carried out according to a fixed transfer velocity  
6 and is assumed to be at equilibrium between the atmospheric layer and the surface water at  
7 the temperature and salinity-dependent saturation level. The solubility of dissolved oxygen  
8 depends on temperature, salinity and pressure (Weiss 1970). The O<sub>2</sub> flux into the atmosphere  
9 is neglected since the atmospheric concentration of O<sub>2</sub> is by far larger than the DO  
10 concentration at the ocean surface.

11 The temperature-dependent annual export production of particulate organic carbon (POC) and  
12 opal from the euphotic zone is calculated via Michaelis-Menten kinetics (Parsons and  
13 Takahashi 1973) and CaCO<sub>3</sub> production is dependent on the particulate organic and opal  
14 production. This relationship is based on the assumption that in the present day ocean there is  
15 a dominance of the silicate producers (e.g. diatoms) over the calcareous plankton (e.g.  
16 coccolithophores) (Falkowski et al. 2007). The POC export from the surface into the deep sea  
17 is determined from organic carbon production in the uppermost layer and then transported to  
18 the deep with a uniform sinking rate of 120 m day<sup>-1</sup>. Remineralization of organic matter  
19 depends on the availability of oxygen for consumption in the water column. Remineralization  
20 of POC occurs as long as dissolved O<sub>2</sub> is larger than the minimum O<sub>2</sub> concentration [O<sub>2min</sub>] =  
21 10<sup>-5</sup> mol L<sup>-1</sup> for bacterial decomposition of POC. A more detailed description of the model  
22 can be found elsewhere (Maier-Reimer and Hasselmann 1987, Heinze et al. 1991, Maier-  
23 Reimer and Heinze 1999, Heinze et al. 1999, Palastanga et al. 2011, Palastanga et al. 2013,  
24 Beaty-Sykes 2014).

25

### 26 **3 Experimental Design**

27 The annually averaged version of the model was integrated to quasi-equilibrium state (200  
28 kyr) with a stable atmospheric CO<sub>2</sub> concentration of 279.78 ppmv. The reference experiment  
29 ~~as well as~~ all OMZ sensitivity experiments ~~is~~ ~~are~~ started from the near-equilibrium state  
30 and integrated for 30,000 yrs. For the reference experiment, the model is forced ~~with~~ ~~from~~  
31 ~~flow~~ fields ~~from the a~~ LSG simulation. The globally averaged ~~potential temperature and~~

1 salinity are is potential temperature of 3.78°C and a globally averaged salinity is of 34.8 psu  
2 respectively (Winguth et al. 1999).

3 Carbon cycle sensitivity experiments are conducted in ~~two~~ three sets of scenarios. The first set  
4 of scenarios consists of a perturbation of the atmospheric CO<sub>2</sub> concentration relative to  
5 preindustrial atmospheric levels ( $pCO_{2ref}$ , PAL) of 2 X CO<sub>2</sub>, 4 X CO<sub>2</sub>, 6 X CO<sub>2</sub>, and 8 X CO<sub>2</sub>  
6 to explore the sensitivity of distribution of dissolved oxygen concentration to rising  
7 atmospheric pCO<sub>2</sub> level. In these simulations, all other boundary conditions and model  
8 parameters are kept at preindustrial levels (Table 1). In a second set of experiments the pCO<sub>2</sub>  
9 levels are accompanied by the associated changes of temperature at the sea surface as well as  
10 in the deep sea to investigate the response of the dissolved oxygen distribution to increases in  
11 CO<sub>2</sub> radiative forcing. In a third set of experiments: POC is kept at preindustrial level to  
12 explore the relative strength of loss of O<sub>2</sub> solubility and oxygen consumption by  
13 remineralization. The preindustrial POC experiments are simulated with at atmospheric CO<sub>2</sub>  
14 concentrations of 2 X, 4 X and 8 X CO<sub>2</sub>. Stabilization scenarios and brief descriptions are  
15 listed in Table 2.

16 In ~~the~~ all CO<sub>2</sub> perturbation scenarios atmospheric pCO<sub>2</sub> is increased from preindustrial levels  
17 by 1% each year (t) until the perturbed atmospheric pCO<sub>2</sub> ( $pCO_{2pert}$ ) is stabilized at its  
18 maximum level ( $pCO_{2max}$ ) by

$$\begin{aligned} & \text{for } pCO_2 < pCO_{2max}: pCO_{2pert} = pCO_{2ref}(1 + 0.01)^t \\ & \text{and for } pCO_2 \geq pCO_{2max}: pCO_{2pert} = pCO_{2max}. \end{aligned} \quad (1)$$

21 The 1% increase of atmospheric CO<sub>2</sub> concentration follows the IPCC (2013) business as usual  
22 scenario and is stabilized after 70 years for doubling of preindustrial pCO<sub>2</sub> (see also Winguth  
23 et al. 2005). The second set of carbon perturbation scenarios includes the feedback of  
24 increasing seawater temperature due to rising atmospheric pCO<sub>2</sub> (Fig. 1). Temperature  
25 increases as a function of the 1% increase per time step of atmospheric pCO<sub>2</sub> and is  
26 determined using Eq. 2 from Hansen et al., (1988) for the radiative forcing of CO<sub>2</sub> with the  
27 addition of a climate model sensitivity of  $A_T=0.6870$ .

$$\Delta T = A_t 6.3 \ln\left(\frac{pCO_2}{pCO_{2ref}}\right) \quad (2)$$

29 Therefore a doubling of pCO<sub>2</sub> results in a homogeneous increase in temperature of ~3°C,  
30 which is consistent with the estimate of Archer (2005) and Hansen et al. (1988). Note that this

1 enhanced sensitivity includes climate feedbacks whereas the direct CO<sub>2</sub> warming for 2 X CO<sub>2</sub>  
2 is ~1.2°C (Ruddiman 2001, Houghton 2004). The resultant temperature change of the ocean  
3 for the doubling of pCO<sub>2</sub> for 2 X CO<sub>2</sub>, 4 X CO<sub>2</sub>, 6 X CO<sub>2</sub>, and 8 X CO<sub>2</sub> is 2.8°C, 5.9°C,  
4 8.7°C, and 11.5°C respectively (Fig. 1). The temperature change is applied at all depths of the  
5 ocean. Solubility and chemical kinetic equilibrium constants of the carbon cycle are adjusted  
6 to the changes in pCO<sub>2</sub> and temperature at each time step in the temperature feedback  
7 experiments.

8 In addition to experiments with increased pCO<sub>2</sub> with and without radiative forcing a reduced  
9 biology scenario is added in which primary productivity and export (Si, CaCO<sub>3</sub>, and organic  
10 carbon) is set to zero following the approach of Maier-Reimer et al. (1996). The reduced  
11 biology scenario is simulated with preindustrial pCO<sub>2</sub> (279 ppmv; Table 2).

12 ~~In addition to Another scenario with experiments with increased pCO<sub>2</sub> with and without~~  
13 ~~radiative forcing absolutely depleted primary and export production (Si, CaCO<sub>3</sub>, and organic~~  
14 ~~carbon) and a preindustrial pCO<sub>2</sub> values (279 ppmv; Table 2) reduced biology scenario has~~  
15 ~~been carried out is added in which primary productivity and export (Si, CaCO<sub>3</sub>, and organic~~  
16 ~~carbon) is set to zero following the approach of Maier-Reimer et al. (1996). The reduced~~  
17 ~~biology scenario is simulated with preindustrial pCO<sub>2</sub> (279 ppmv).~~

18 Four additional simulations were conducted in order to explore how DO concentrations in the  
19 model respond to changes in ocean ventilation. Velocity variables w, v and u are reduced  
20 uniformly over the ocean globally by 25%, 50%, 75% and 100%. Convection and diffusion  
21 are not changed in these experiments and remain at preindustrial values.

22 ~~In addition to experiments with increased pCO<sub>2</sub> with and without radiative forcing a reduced~~  
23 ~~biology scenario is added in which primary productivity and export (Si, CaCO<sub>3</sub>, and organic~~  
24 ~~carbon) is set to zero following the approach of Maier-Reimer et al. (1996). The reduced~~  
25 ~~biology scenario is simulated with preindustrial pCO<sub>2</sub> (279 ppmv).~~

26

## 27 **4 Results**

### 28 **4.1 Reference simulation**

29 The relevant results of the reference experiment will be briefly discussed in this section.  
30 Prescribed temperature and salinity taken from Winguth et al. (1999) are comparable to the

Formatted: Subscript

1 observed data from the World Ocean Atlas 2013 (referred hereafter as WOA2013; Locarnini  
2 et al. 2013, Zweng et al. 2013) and to the simulations of Maier-Reimer (1993). Simulated  
3 seawater temperature, dissolved oxygen, and salinity are comparable to the World Ocean  
4 Atlas 2013 at 3000 m depth (Fig. 2). Due to the slow ventilation of the ocean the WOA2013  
5 data at 3000 m is more representative of preindustrial conditions. Compared to WOA2013,  
6 cooler simulated temperatures are projected for the Bering Sea by the LSG, leading to greater  
7 O<sub>2</sub> solubility at the surface and therefore higher DO concentration than the corresponding data  
8 from WOA2013 (Garcia et al. 2013, Locarnini et al. 2013). This bias may be partially linked  
9 to the long-term warming trend over the last decades (IPCC, 2013). Dissolved inorganic  
10 carbon (DIC) at the surface is similar to the simulations of Maier-Reimer (1993) and the  
11 observations from the WOA2013 (Locarnini et al. 2013) with the exception of the Arctic  
12 region in which the reference experiment simulated DIC concentrations at approximately 150  
13  $\mu\text{mol kg}^{-1}$  less compared to corresponding values simulated by Maier-Reimer (1993). The  
14 decreased simulated DIC in the Arctic region of this preindustrial simulation could be due to  
15 the addition of dust fields (Mahowald et al. 2006) and Fe and P cycles (Palastanga et al. 2011,  
16 Palastanga et al. 2013). Simulated ocean oxygen concentrations are comparable to Maier-  
17 Reimer (1993) and the WOA2013. POC, CaCO<sub>3</sub>, and opal export and sediment composition  
18 are comparable to Maier-Reimer (1993). However, the model does trend toward a slightly  
19 higher POC in the tropical latitudes compared to Sarmiento and Gruber (2006) who used the  
20 chlorophyll concentration and sea surface temperature based empirical algorithm of Dunne et  
21 al. (2005). This bias may be linked to overestimation of export production in HAMOCC 2.0  
22 linked to nutrient trapping (Najjar et al. 1992) at the equator region of the Pacific Ocean (Fig.  
23 2). In addition, HAMOCC 2.0 simulates a slightly elevated export of CaCO<sub>3</sub> and opal export  
24 compared to corresponding observed values inferred from CaCO<sub>3</sub>:POC and opal:POC export  
25 ratios (Sarmiento and Gruber 2006) (2006) who used the chlorophyll concentration and sea  
26 surface temperature based empirical algorithm of Dunne et al. (2005). This bias may be linked  
27 to overestimation of export production in HAMOCC 2.0 linked to nutrient trapping (Najjar et  
28 al. 1992) at the equator region of the Pacific Ocean (Fig. 2). In addition, HAMOCC 2.0  
29 simulates a slightly elevated export of CaCO<sub>3</sub> and opal export compared to corresponding  
30 observed values inferred from CaCO<sub>3</sub>:POC and opal:POC export ratios (Sarmiento and  
31 Gruber 2006).

Formatted: Font:

Formatted: Highlight

Formatted: Font:

Formatted: Subscript

Formatted: Subscript

Formatted: Font: (Default) Arial

## 4.2 Model representation of the oxygen minimum zones in the reference simulation

Simulated DO distribution in the reference simulation represents all five major non-seasonal oxygen minimum zones of the Pacific Ocean and Indian Ocean and the seasonal OMZ or low oxygen zone (LOZ; defined as dissolved  $[O_2] < 90 \mu\text{mol kg}^{-1}$ ) of the eastern South Atlantic Ocean (Fig. 3). However, due to the coarse model grid, the eastern subtropical and tropical North Pacific OMZ as well as the OMZs in the Indian Ocean (Arabian Sea and Bay of Bengal) are not resolved individually. The LOZ of the eastern South Atlantic Ocean is simulated in the reference experiment with a OMZ core of  $\sim 17\text{-}19 \mu\text{mol kg}^{-1} O_2$  and therefore, following the OMZ definition proposed here, the LOZ of the Atlantic Ocean is simulated as a non-seasonal OMZ.

The simulation is generally agreeable with the extent and depth of the OMZs, and DO core concentration values of the observations (Fig. 3). A model-data bias of the OMZ exist in the North Pacific Ocean resulting in the simulated OMZ reaching too far westward with the western boundary near  $\sim 180^\circ\text{W}$ . The OMZ is also simulated too deep with a maximum depth of approximately 2300m. The difference in horizontal extent between the model simulation and observed in the eastern North Pacific OMZ may be attributed to the non-consideration of seasonally variability in the simulation. For the sub-tropical South Atlantic Ocean, the simulated OMZ core is located in a water depth ranging from 300 to 700 meters; which is slightly shallower than the OMZ core in the Indian Ocean. The total ocean surface area with a DO concentration of  $\leq 20 \mu\text{mol kg}^{-1}$  is approximately 8.6% in the reference simulation and the total ocean volume with DO concentration of  $\leq 20 \mu\text{mol kg}^{-1}$  is approximately 1.4%.

## 4.2 Sensitivity of simulated dissolved oxygen to a reduced ventilation and biological pump

In order to explore the importance of biological pump (soft tissue pump) to the distribution and concentration of dissolved oxygen globally in the ocean we performed experiments in which  $P_{\text{POC}}$  remains at preindustrial levels and atmospheric  $\text{CO}_2$  is increased by 2 X, 4 X and 8 X  $\text{CO}_2$  as well as an extreme scenario in which all productivity is reduced to zero. This extreme simulation, referred hereafter as the reduced biology scenario, is similar to the “Kill Biology” experiment by Maier-Reimer et al. (1996). In this simulation the atmospheric  $p\text{CO}_2$  is set to preindustrial levels, which is in contrast to a simulated exponential increase in

Formatted: Highlight

1 atmospheric pCO<sub>2</sub> in response to the diminished export production in the study of Maier-  
2 Reimer et al. (1996).

3 Due to the reduced export production, the DIC concentrations increase at the ocean surface by  
4 >400 μmol kg<sup>-1</sup> and by >200 μmol kg<sup>-1</sup> in the intermediate and deep-water masses at mid-  
5 latitudes. This leads to a significant rise in total alkalinity by an average of 550 μeq kg<sup>-1</sup>. As a  
6 result, the pH increases by an average of 0.7 units despite the loss of calcification and CaCO<sub>3</sub>  
7 burial. Note that weathering rates are kept at preindustrial conditions in all simulations.  
8 Dissolved oxygen increases by ~150 μmol kg<sup>-1</sup> in the deep-sea and ~200 μmol kg<sup>-1</sup> in the  
9 intermediate water masses. The dissolved oxygen gradient in this reduced biology scenario is  
10 controlled by the air-sea gas exchange of O<sub>2</sub> at the surface and by the temperature-dependent  
11 solubility of oxygen: not by the vertical POC flux, which is set by definition to zero to the  
12 “killed” productivity. Thus consumption of oxygen by decay of POC is also diminished.

13 Experiments were performed to evaluate OMZ response to weakened ventilation (eg. vertical,  
14 zonal and meridional velocities) in the model. Ventilation is decreased by 25%, 50%, 75%  
15 and 100% (Fig. 4). With a 25% decrease the OMZ core (< 25 μmol kg<sup>-1</sup>) the OMZ deepen in  
16 each ocean basin and expand horizontal only slightly. The OMZs continue to expand in the  
17 experiment with 50% reduction in ventilation. Although P<sub>POC</sub> is decreasing as expected with  
18 the reduction in ventilation, DOC increase with a loss of 25% and 50% leading to the  
19 expansion of the OMZs in these two simulation. However, in simulations with 75% or  
20 greater loss in ventilation the DO concentration within the OMZ increases (Fig. 4). The  
21 increase in DO concentration coincides with a loss of P<sub>POC</sub> as well as DOC globally and in  
22 equatorial region. Simulated dissolved oxygen concentrations in the deep sea increase in the  
23 model in each reduced ventilation scenario due to the convection of oxygen at the poles.

#### 24 **4.3 Model sensitivity to changes in oxygen solubility**

25 Solubility is another control of OMZ expansion; therefore, to determine how the model  
26 represents the expansion of OMZs due to solubility in response to radiative forcing, P<sub>POC</sub> is  
27 held at preindustrial levels and atmospheric CO<sub>2</sub> is increased to 2 X, 4 X and 8 X preindustrial  
28 concentrations. Oxygen solubility is dependent on salinity, pressure and temperature and is  
29 calculated using the equation presented by Weiss (1970) yielding an average change of ~0.3  
30 ml L<sup>-1</sup> per doubling of pCO<sub>2</sub> with the most significant changes in the deep sea. The relative  
31 strength of solubility and P<sub>POC</sub> on OMZ expansion will be examined in the discussion.

Formatted: Heading 2

Formatted: Not Highlight

#### 1 **4.34.4 Sensitivity of the OMZs and global dissolved oxygen concentrations to** 2 **increased pCO<sub>2</sub> without radiative forcing**

3 The increased pCO<sub>2</sub> simulations that do not include radiative forcing (temperature increase;  
4 Eq. 2) result in small increases of dissolved oxygen [in the model](#) at the ocean surface due to  
5 the enhancement of primary productivity. The small increase in productivity results in  
6 increased DO globally. There are only slight changes in the distributions of DO concentration  
7 for these simulations as compared to the simulation that include radiative forcing (Fig. 5).  
8 Therefore, in order to discuss future changes in the OMZs the following sections address the  
9 expansion of each OMZ and OMZ core as well as the global change at 2 X, 4 X, 6 X, and 8 X  
10 CO<sub>2</sub> simulations that include the temperature feedback.

#### 11 **4.44.5 Sensitivity of the oxygen minimum zones to CO<sub>2</sub> radiative forcing**

12 In each of the scenarios that include radiative forcing, the simulated OMZs expand ([Fig 6](#)).  
13 The results show the formation of a new OMZ core in the tropical western South Pacific  
14 Ocean. There are significant changes in the distributions of DO concentrations in all  
15 simulations.

#### 17 **4.4.24.5.1 Simulated OMZ expansion in the eastern tropical Pacific Ocean in** 18 **response to CO<sub>2</sub> radiative forcing**

19 For the 2 X CO<sub>2</sub> experiment, the OMZ cores (dissolved O<sub>2</sub> concentration  $\leq 20 \mu\text{mol } \mu\text{kg}^{-1}$ ) of  
20 the OMZ in the eastern North Pacific Ocean expands to 65°N compared to the extent to 35°N  
21 of corresponding OMZ in the 1 X CO<sub>2</sub> scenario. This OMZ merges with that of the eastern  
22 South Pacific OMZ at the equator and therefore is considered as a single OMZ, hereafter  
23 referred to as the eastern Pacific OMZ ([Fig. 6](#)). At a depth of 450 m it extends northward  
24 around the northern boundary of the North Pacific gyre with dissolved oxygen concentrations  
25 of  $\leq 20 \mu\text{mol O}_2 \mu\text{kg}^{-1}$  in the Gulf of Alaska. The southern boundary of the eastern Pacific  
26 OMZ is located near the coast of Northern Chile at approximately 30°S at 450 meters depth.  
27 Compared to the reference simulation, the OMZ in the 2 X CO<sub>2</sub> experiment expands 200 km  
28 further to the south. The OMZ western boundary increases by approximately 550 km to  
29 150°E. The depth of hypoxia (DOH) is between 150-250 meters. The OMZ has a max depth  
30 of 1900 meters, 200 meters deeper than the reference simulation ([Fig. 6](#)). The OMZ core

1 shoals to 380 meters; however, ~~#the bottom boundary of the OMZ core~~ does not deepen in  
2 the 2 X CO<sub>2</sub> simulation. The lowest oxygen concentration in the OMZ core is 17 μmol O<sub>2</sub> kg<sup>-1</sup>  
3 in this simulation (Fig. 7).

4 The horizontal extent of the OMZ in the 4 X CO<sub>2</sub> scenario is similar to the 2 X CO<sub>2</sub>  
5 experiment with the addition of all of the North Pacific outside of the North Pacific Gyre  
6 having a dissolved oxygen concentration of ≤50 μmol L<sup>-1</sup> at a depth of 450 meters (Fig. 6).

7 The depth of hypoxia shoals vertically to between 75-150 m from the surface in the North  
8 Pacific Ocean and remains in a depth range of 150-250 m in the South Pacific Ocean. The  
9 maximum depth of the Pacific OMZ increases to 2000 m. For the 4 X CO<sub>2</sub> experiment, the  
10 OMZ core extends ~100 km west and deepens by 200 m compared to the 2 X CO<sub>2</sub>  
11 simulations. The depth of the OMZ core does not change in the 4 X CO<sub>2</sub> simulations  
12 compared to the 2 X CO<sub>2</sub> simulations; however, the minimum dissolved oxygen concentration  
13 decreases to 14 μmol kg<sup>-1</sup> (Fig. 47).

14 There is further extension of the OMZ core south to approximately 50°S (central coast of  
15 Chile) at 450 m depth in the 8 X CO<sub>2</sub> scenario relative to the 4 X CO<sub>2</sub> experiment (Fig. 6).

16 The OMZ core, at a depth of ~2000 meters, does not shoal or deepen in the 6 X and 8 X CO<sub>2</sub>  
17 compared to the 4 X CO<sub>2</sub> experiment. In the 8 X CO<sub>2</sub> simulation, the core becomes hypoxic  
18 with a minimum dissolved oxygen concentration of ≤8 μmol kg<sup>-1</sup>. The 6 X CO<sub>2</sub> experiment  
19 results in a minimum dissolved oxygen concentration of ~12 μmol kg<sup>-1</sup> (Fig. 47).

#### 20 4.4.34.5.2 Simulated OMZ expansion in the eastern tropical South Atlantic 21 Ocean in response to CO<sub>2</sub> radiative forcing

22 The horizontal expansion of the OMZ in the eastern South Atlantic in the 2 X CO<sub>2</sub> simulation  
23 remains similar to the reference scenario with a southern boundary at approximately 25°S and  
24 extends northward along the west coast of Africa to the southern tip of Morocco to  
25 approximately 15°N (Fig. 6). The depth of hypoxia shoals from between 250-450 m in the  
26 reference experiment to 150-250 m. The maximum depth of OMZ increases by 100 m to 1200  
27 m. In the eastern South Atlantic, the OMZ core in the 2 X CO<sub>2</sub> experiment expands relative to  
28 the reference experiment southward by 580 km to approximately 19°S and northward by 110  
29 km (~1° northward propagation). In the 2 X CO<sub>2</sub> experiment, the OMZ core expands  
30 vertically; it shoals to 450 m and deepens to 915 m, which is 65 m deeper than the reference

1 simulation. The minimum dissolved O<sub>2</sub> concentration is reduced by 1 μmol kg<sup>-1</sup> relative to  
2 the reference experiment to 17 μmol O<sub>2</sub> kg<sup>-1</sup> (Fig. 7).

3 Relative to the reference simulation, the 4 X CO<sub>2</sub> simulation results in insignificant horizontal  
4 expansion of the OMZ in the latitudinal direction (Fig. 6). The most notable area of expansion  
5 of the OMZ is in the southwest direction in which the southwestern boundary of the eastern  
6 South Atlantic OMZ extends to ~30°S and ~20°W. The maximum depth increases by an  
7 additional 100 m to a depth of 1300 m. The OMZ core expands symmetrically in east-west  
8 direction, by about 100 km, encompassing the Gulf of Guinea. The vertical expansion of the  
9 OMZ core is negligible between the 2 X and 4 X CO<sub>2</sub> simulations; however, the strength of  
10 the core increases significantly with a minimum dissolved O<sub>2</sub> concentration of 12 μmol kg<sup>-1</sup>  
11 (Fig. 47).

12 Horizontal expansion of the eastern South Atlantic OMZ does not occur between the 4 X CO<sub>2</sub>  
13 simulation and the 6 X or 8 X CO<sub>2</sub> scenarios (Fig. 6). In the 6 X CO<sub>2</sub> scenario the horizontal  
14 extent of the eastern South Atlantic Ocean at 450 m depth is reduced from the 4 X CO<sub>2</sub>  
15 simulation, where as in the 8 X CO<sub>2</sub> simulation the horizontal area expands back to the extent  
16 of the 4 X CO<sub>2</sub> simulation. The depth of hypoxia remains between 150-250 m depth for both  
17 6 X and 8 X CO<sub>2</sub> experiments. The maximum depth of the OMZ increases to 1500 m in the 8  
18 X CO<sub>2</sub> simulation. The OMZ core deepens to 1050 m and shoals from the 6 X and 8 X CO<sub>2</sub>  
19 scenarios to 375 m. The minimum dissolved O<sub>2</sub> concentration remains at 12 μmol L<sup>-1</sup> for both  
20 the 6 X and 8 X CO<sub>2</sub> simulations (Fig. 47).

#### 21 4.4.44.5.3 Simulated expansion of the OMZ in the tropical Indian Ocean in 22 response to CO<sub>2</sub> radiative forcing.

23 The expansion of the OMZ in the Indian Ocean is limited at the western boundary by the east  
24 coast of Africa and the eastern boundary is constrained by the Indonesian archipelago. The  
25 Indian Ocean OMZ includes the poorly resolved Arabian Sea and the Gulf of Bengal, which  
26 is limited by the Indian subcontinent. Compared to the reference simulation, the OMZ extends  
27 southward to 10°S in the 2 X CO<sub>2</sub> simulation and deepens by 100 m to 1100 m (Fig. 6). The  
28 OMZ core does not expand horizontally but deepens to 900 meters and shoals by 50m to 225  
29 meters. The minimum dissolved oxygen concentration is 10 μmol kg<sup>-1</sup> and remains the  
30 lowest concentration for each of the emissions scenario (Fig. 47).

1 In the 4 X, 6 X, and 8 X pCO<sub>2</sub> simulations the horizontal expansion in the Indian Ocean OMZ  
2 is insignificant but it deepens to 1300 m, 1400 m, 1700 m, respectively. For the 4 X CO<sub>2</sub>  
3 experiment the OMZ core expands in the western direction to 45°E and deepens by 100 m to  
4 1000 m; however, the upper boundary of the OMZ remains unchanged. In the 8 X CO<sub>2</sub>  
5 simulation the core expands southward by 650 km to approximately 16°S and shoals to 100 m  
6 for both the 6 X and 8 X CO<sub>2</sub> scenarios; however, the lower boundary remains unchanged  
7 compared to the 4 X CO<sub>2</sub> experiment. The depth of hypoxia is located between 25 m and 75  
8 m in the reference experiment and in all CO<sub>2</sub> emission scenarios. It is important to note that  
9 due to complex climate variability and nutrient trapping the annual tracer distribution in the  
10 Indian Ocean consist of large uncertainties and thus the model-data bias is generally high in  
11 the region.

#### 12 4.4.5.4 Simulated OMZ formation in the western tropical Pacific Ocean in 13 response to CO<sub>2</sub> radiative forcing

14 An OMZ core (<20 μmol L<sup>-1</sup> O<sub>2</sub>) is simulated in the western tropical Pacific Ocean (143E,  
15 2N) near the Bismarck Sea (Fig. 6 and 58). This region is modeled as a low oxygen zone  
16 (LOZ) in the reference simulation. For the 4 X CO<sub>2</sub> experiment, the OMZ develops in <2000  
17 yr integration with a minimum dissolved oxygen concentration of 17 μmol L<sup>-1</sup>. The upper  
18 boundary of the OMZ core remains unchanged for all perturbation simulations compared to  
19 the reference. However, the OMZ core deepens from 725 m at 3 X CO<sub>2</sub> to 1000 m for the 8 X  
20 CO<sub>2</sub> simulation.

#### 21 4.54.6 Export of particulate organic carbon and changes in global dissolved O<sub>2</sub> 22 concentration in response to simulations with CO<sub>2</sub> radiative forcing

23 Simulated Total POC production and export production of POC (P<sub>POC</sub>) from the euphotic  
24 zone into the deep sea increases predominantly near the equatorial Pacific with a rise in  
25 seawater temperature in response to CO<sub>2</sub> radiative forcing (Fig. 2). P<sub>POC</sub> in the northern Indian  
26 and western tropical Pacific decreases in response to enhanced CO<sub>2</sub> radiative forcing most  
27 likely due to nutrient trapping in the eastern Pacific Ocean; ~~where as~~ changes P<sub>POC</sub> in the  
28 east Atlantic Ocean are insignificant.

29 Global DO concentration decreases most rapidly during the first 2000 years of integration in  
30 each carbon perturbation simulation. The reduction in global dissolved oxygen concentration

Formatted: Subscript

1 continues on average 1500 years beyond the year in which the peak pCO<sub>2</sub> emission value is  
2 reached. The total ocean area with a dissolved oxygen concentration of <50 μmol kg<sup>-1</sup>  
3 expands at approximately 2% per ~3°C increase in seawater temperature which corresponds  
4 to a doubling of pCO<sub>2</sub>. The total ocean area volume at which the dissolved O<sub>2</sub> concentration is  
5 <50 μmol kg<sup>-1</sup> increases by 107.5% in the 8 X CO<sub>2</sub> simulations. The increase in the ocean  
6 volume of of hypoxic area water in to the photic zone is insignificant (< 0.3%) due to the  
7 equilibrium of oxygen between the atmosphere and the surface layer in the model air-sea gas  
8 exchange. However, an area of hypoxia forms in the photic zone of the sub-tropical North  
9 Pacific Ocean with a dissolved O<sub>2</sub> concentration of less than 12 μmol kg<sup>-1</sup>.

#### 10 ~~4.5 Sensitivity of dissolved oxygen to changes in solubility and reduced~~ 11 ~~biological pump and atmospheric oxygen concentration~~

12 ~~In order to explore the importance of biological pump (soft tissue pump) to the distribution~~  
13 ~~and concentration of dissolved oxygen globally in the ocean we performed an additional~~  
14 ~~experiments in which P<sub>POC</sub> remains at preindustrial levels and atmospheric CO<sub>2</sub> is increased~~  
15 ~~by 2 X, 4 X and 8 X CO<sub>2</sub> as well as an extreme scenario in which all productivity is reduced~~  
16 ~~to zero. This extreme simulation, referred hereafter as the reduced biology scenario, is similar~~  
17 ~~to the “Kill Biology” experiment by Maier Reimer et al. (1996). In this simulation the~~  
18 ~~atmospheric pCO<sub>2</sub> is set to preindustrial levels, which is in contrast to a simulated exponential~~  
19 ~~increase in atmospheric pCO<sub>2</sub> in response to the diminished export production in the study of~~  
20 ~~Maier Reimer et al. (1996).~~

#### 21 ~~— Sensitivity of dissolved oxygen in Oxygen Minimum Zones to changes in~~ 22 ~~oxygen solubility~~

Formatted: Heading 3

#### 24 ~~— Sensitivity of simulated global dissolved oxygen to a reduce biological~~ 25 ~~pump~~

Formatted: Heading 3

26 ~~Due to the reduced export production, the DIC concentrations increase at the ocean surface by~~  
27 ~~>400 μmol kg<sup>-1</sup> and by >200 μmol kg<sup>-1</sup> in the intermediate and deep water masses at mid-~~  
28 ~~latitudes. This leads to a significant rise in total alkalinity by an average of 550 μeq kg<sup>-1</sup>. As a~~  
29 ~~result, the pH increases by an average of 0.7 units despite the loss of calcification and CaCO<sub>3</sub>~~  
30 ~~burial. Note that weathering rates are kept at preindustrial conditions in all simulations.~~

1 Dissolved oxygen increases by  $\sim 150\text{--}300\ \mu\text{mol kgL}^{-1}$  in the deep sea and  $\sim 200\ \mu\text{mol kgL}^{-1}$   
2 in the intermediate water masses. The dissolved oxygen gradient in this reduced biology  
3 scenario is controlled by the air-sea gas exchange of  $\text{O}_2$  at the surface and by the temperature-  
4 dependent solubility of oxygen: not by the vertical POC flux, which is set by definition to  
5 zero to the “killed” productivity. Thus consumption of oxygen by decay of POC is also  
6 diminished (Fig. 6). In an additional experiment, the sensitivity of deep-sea dissolved oxygen  
7 concentration to changes in atmospheric  $\text{O}_2$  concentration is explored by reducing the  
8 atmospheric  $p\text{O}_2$  by 50%. The decrease in atmospheric  $p\text{O}_2$  does not alter the dissolved  
9 oxygen concentration significantly compared to the reference experiment.

## The response of simulated dissolved oxygen concentrations to reduced ventilation

Formatted: Heading 2

## 5 Discussion

14 In this study we investigate the expansion of OMZ in a biogeochemical model as a result of  
15 seawater temperature increase in response to  $\text{CO}_2$  radiative forcing and changes in  $P_{\text{POC}}$  in a  
16 biogeochemical model. It is important to note that changes in ocean stratification due to ocean  
17 temperature and density changes are not simulated and held constant at preindustrial  
18 conditions to allow for the long-term carbon cycle feedback and an integration time of 30  
19 kyrs. The focus of this study is to examine changes in OMZs due to changes in solubility and  
20 productivity/remineralization. Furthermore, this study determines the relative strengths of  
21 these two mechanisms of OMZ expansion in the biogeochemical model. Therefore,  
22 the expansion of OMZs in this study are the result of changes in  $\text{O}_2$  solubility and  
23 temperature-dependent productivity and changes in in  $\text{O}_2$  solubility; therefore consequently,  
24 OMZ expansion may be modest due to no consideration of a weakened connection between  
25 the OMZ and the ocean surface in the future (Glessmer et al. 2011). It has been suggested that  
26 the depth and strength of the thermocline may influence OMZ expansion and contraction  
27 (Deutsch et al. 2007). An increase of the thermocline in a warmer climate may result in a  
28 contraction of the OMZs due to reduced oxidative demand in hypoxic waters. However, this  
29 study assumes a constant thermocline depth, as the temperature increase is uniform at all  
30 depths. Other assumptions in this study are a constant nutrient inventory and Redfield ratio as  
31 well as a constant rate of denitrification. Changes in the elemental stoichiometry (carbon

1 overconsumption) due to rising pCO<sub>2</sub> has been suggested as a possible mechanism of  
2 enhanced volume of suboxic water in the ocean due to the respiration of increased organic  
3 carbon (Oschlies et al. 2008, Riebesell et al., 2007). Measurements of dissolved oxygen  
4 concentration in the suboxic regions of the oceans are limited (Levitus et al. 2013, Locarnini  
5 et al. 2006); however, paleo-records and climate models support the assumption that ocean  
6 anoxic events occur during periods of high pCO<sub>2</sub> (Knoll et al., 1996; Falkowski et al. 2011).  
7 Furthermore, OMZs have expanded and contracted during the glacial interglacial cycles  
8 (Galbraith et al. 2004) as well as on shorter time scales in response to Dansgaard-Oeschger  
9 (D-O) events (Cannariato and Kennett 1999).

10 In the ventilation scenarios the model responds as expected for the reductions in ocean  
11 ventilation of 75% or greater. Figure 4 illustrates the dissolved oxygen response to a near  
12 complete shutdown of ocean ventilation resulting in an increase in the vertical oxygen  
13 gradient relative to the reference scenario—slightly stratified oxygen profile. The increase in  
14 DO in the reduced ventilation simulations of greater than 75% are due to the reduced P<sub>POC</sub> and  
15 thus reduced remineralization and to the convection of DO to the deep sea at the poles. The  
16 expansion of OMZ cores at lower changes in ventilation (eg. 25% and 50%; Fig 4) may be  
17 due the increase of DOC both global and regionally. An increase in dissolved organic carbon  
18 results in more available DO for remineralization in the model; therefore, even with reduced  
19 P<sub>POC</sub> the model response to atmospheric perturbations with an expansion of OMZs with a 25%  
20 and 50% reduction in ventilation.

21 The comparison between the 25% and 50% reduced ventilation experiment and the 4 X CO<sub>2</sub>  
22 with radiative forcing simulation, specifically in the Pacific Ocean basin, indicates that the  
23 decrease of dissolved oxygen concentration in the model is strongly controlled by P<sub>POC</sub> and  
24 solubility as the expansion is greater due to the influence of these mechanisms rather than a  
25 25% reduction in ocean ventilation or the increase in DOC (Fig. 9). This dominant strong  
26 control by remineralization of organic matter in comparison to ventilation changes may be  
27 link to changes in upwelling and export production.

28 The increased atmospheric CO<sub>2</sub> with radiative forcing simulations of this study agree with  
29 other studies of model-simulated change and observed change in the extent of OMZs  
30 (Whitney et al. 2007, Karstensen et al. 2008, Stramma et al. 2008, Shaffer et al. 2009,  
31 Falkowski et al. 2011). However, the simulations presented here have a greater overall  
32 decrease in global oxygen concentration of 9.1% after 300 years of integration for a doubling

Formatted: Not Highlight  
Formatted: Not Highlight  
Formatted: Not Highlight  
Formatted: Not Highlight

1 of pCO<sub>2</sub> than previous studies, which range from 1-7% for various pCO<sub>2</sub> emissions and  
2 integration times (Matear et al. 2000, Bopp et al. 2002, Oschlies et al. 2008, Schmittner et al.  
3 2008, Bopp et al. 2013). The rapid decrease in global dissolved O<sub>2</sub> concentration is due to the  
4 rapid change in global ocean temperature linked to the 1% business as usual atmospheric CO<sub>2</sub>  
5 emissions. However, the dissolved oxygen concentrations in the OMZ areas decrease more  
6 slowly in the model simulations as compared to the observed trends from Stramma et al.,  
7 (2008). The study of Stramma et al., (2008) suggests a temperature increase of 0.005 °C yr<sup>-1</sup>  
8 in the Atlantic and Indian Oceans and a temperature decrease by 0.005 °C yr<sup>-1</sup> for the Pacific  
9 Ocean since the 1960s. Most of the expansion of suboxic area in this model study occurs  
10 during the first 2000 years of the 30,000-year simulation due to the slow response time,  
11 particularly in the deep Pacific Ocean. The atmospheric pCO<sub>2</sub> is stabilized at the elevated CO<sub>2</sub>  
12 concentrations in the carbon perturbation simulations in this study; therefore, no recovery is  
13 simulated.

14 In all carbon perturbation simulations the upper boundary of the OMZ cores are  
15 shallower compared to the reference simulation. The shallowest OMZ core is found in the  
16 Indian Ocean OMZ at ~75 meters. Note that the upper boundary of the OMZ is located at 75  
17 m depth because above this depth water masses are influenced by the air sea gas exchange of  
18 the uppermost model layer. The core is not expected to shoal beyond 50 m depth in the  
19 simulations due to the assumption that the ~~atmosphere is at ocean surface oxygen~~  
20 ~~concentration is at~~ equilibrium with the ~~surface of the ocean which is~~ atmosphere and the  
21 simulated ~~surface layer of~~ the top 50 meters. The OMZ core of the North Pacific Ocean has  
22 the deepest upper boundary, shoaling approximately 100 meters for the highest pCO<sub>2</sub> carbon  
23 perturbation scenario. ~~The slower shoaling of the OMZ in the tropical Pacific Ocean~~  
24 ~~compared to that of the tropical eastern Atlantic and Indian Ocean OMZs may be related to~~  
25 ~~difference in solubility as well as linked to a stronger upwelling in the tropical eastern Pacific~~  
26 ~~Ocean. Stronger upwelling in the tropical Pacific Ocean could transport high nutrient and~~  
27 ~~oxygen depleted water masses to the surface; however, in the model these water are at~~  
28 ~~equilibrium with atmosphere and therefore the effect of upwelling on DO concentration is~~  
29 ~~diminished in the model.~~ Downward expansion of the OMZ core is limited by the lower  
30 boundary of the activity-ventilated zone at approximately 2000 meters in the Pacific Ocean.  
31 This depth coincides with the depth of the wind-driven circulation, which remains unchanged  
32 in each simulation, because the same wind stress forcing is applied to all simulations.  
33 Deepening of the eastern South Atlantic OMZ and the Indian Ocean OMZ are also limited to

1 the bottom boundary of the well-ventilated mixed layer (~1500 meter for the Atlantic and  
2 ~1000 meters for the Arabian Sea). The ventilation depth of the Arabian Sea may be  
3 overestimated in the model due to the lack of monsoon variation, which can cause the mixed  
4 layer depth to vary greatly in the Arabian Sea.

5 ~~The simulated OMZs in the Indian and Atlantic Ocean respond to changes in the temperature-~~  
6 ~~dependent export production of POC and to changes in dissolved organic carbon.~~~~The~~  
7 ~~expansion of the OMZ in the Indian Ocean and eastern South Atlantic Ocean are controlled~~  
8 ~~primarily by changes in temperature dependent oxygen solubility and to a lesser extent~~  
9 ~~changes in the temperature dependent export production of POC.~~~~P<sub>POC</sub> increased in the Indian~~  
10 ~~and Atlantic Ocean in the 2 X and 4 X CO<sub>2</sub> simulations and started to decrease in the 6 X and~~  
11 ~~8 X CO<sub>2</sub> experiments (Fig. 2); however, dissolved organic carbon increases at higher pCO<sub>2</sub>~~  
12 ~~concentrations. The decrease in P<sub>POC</sub> may be due to the trapping of nutrients in the equatorial~~  
13 ~~Pacific Ocean which exhibited a large increase in PO<sub>4</sub> at 6 X and 8 X CO<sub>2</sub>. The limited~~  
14 ~~expansion of the OMZ in the Indian and Atlantic Ocean in the 6 X and 8 X CO<sub>2</sub> simulations~~  
15 ~~are the result of oxygen loss due to changes in solubility and to a lesser degree increased~~  
16 ~~dissolved organic carbon, which increases the amount of oxygen available for~~  
17 ~~remineralization by the model (Fig. 10). Therefore, oxygen is still consumed in the OMZs of~~  
18 ~~the Indian Ocean and Atlantic Ocean despite the loss of P<sub>POC</sub> due to the high amount of~~  
19 ~~dissolved organic carbon. Figure 10 shows an increase in mineralization in the Indian and~~  
20 ~~Atlantic Ocean due to high concentration of DOC regardless of the loss in P<sub>POC</sub>. Furthermore,~~  
21 ~~the extent of the OMZs in the Indian Ocean and Atlantic Oceans appears to be insensitive~~  
22 ~~responding to changes in the export of organic matter in response to radiative forcing as well~~  
23 ~~as changes in DOC in simulations of less than 6 times of the preindustrial pCO<sub>2</sub> (Fig 11).~~

24 ~~Figure 7 displays the increase in outgassing of oxygen at higher pCO<sub>2</sub> levels throughout the~~  
25 ~~tropical regions. The water masses of the present day Arabian Sea and Bay of Bengal are~~  
26 ~~much lower in sea surface dissolved oxygen than either the tropical Atlantic or tropical~~  
27 ~~Pacific OMZs and exhibits a shallower depth of hypoxia. Therefore, any further loss of~~  
28 ~~solubility due to ocean warming would cause an intensification of the OMZ. Findings from~~  
29 ~~this sensitivity study suggest that the expansion of the Indian Ocean OMZ in the model is~~  
30 ~~controlled by solubility changes rather than changes in the export production of POC. The~~  
31 ~~simulated extent of the OMZ in the eastern tropical South Atlantic intensifies mainly due to~~  
32 ~~the change in solubility and exhibits the greatest change in sea surface dissolved oxygen~~  
33 ~~concentration due to CO<sub>2</sub> forcing of all the OMZs simulated. There is an insignificant change~~

Formatted: Not Highlight

Formatted: Not Highlight

Formatted: Not Highlight

1 ~~an export production of POC in the eastern tropical South Atlantic OMZ~~ The extent of the  
2 present day OMZ in the Atlantic Ocean has a much higher dissolved oxygen concentration  
3 due to cooler water masses than in the northern Indian Ocean. However, the higher salinity of  
4 the Atlantic Ocean could leads to greater loss of O<sub>2</sub> solubility at higher seawater surface  
5 temperatures as compared to the Indian Ocean or eastern tropical Pacific Ocean for each  
6 pCO<sub>2</sub> simulation.

7 The change in the extent of the OMZ in the Pacific Ocean is driven by the change in  
8 productivity and export production of POC and increases in remineralization (Fig. 10 and  
9 11) ~~and to a lesser degree by changes in temperature dependent dissolved O<sub>2</sub> solubility. The~~  
10 response of the model to changes in P<sub>POC</sub> in the Pacific Ocean is stronger than to a reduction  
11 in ventilation by 25% (Fig. 9). Loss of solubility is greater in the eastern South Atlantic;  
12 ~~however, t~~The increase of export production of POC in the eastern equatorial Pacific OMZ  
13 leads to significant horizontal expansion, which is not simulated in the eastern South Atlantic  
14 or the Indian Ocean OMZs. The model does not indicate a more significant increase in export  
15 production of POC in the cold tongue of the Pacific Ocean as compared to the warm pool in  
16 the western Pacific Ocean. However, it is important to note that the simulated CO<sub>2</sub>-induced  
17 seawater temperature change is uniform and therefore the eastern Pacific seawater  
18 temperature remains cooler relative to other regions of the Pacific Ocean. The Pacific Ocean  
19 OMZ does not shoal as significantly as the Indian Ocean or eastern South Atlantic OMZs but  
20 expands horizontally under the area of high productivity. Oxygen loss due to remineralization  
21 of organic matter is potentially the main mechanism for simulated expansion of the OMZ in  
22 the tropical Pacific Ocean in the model. Figures 8-10 and 11 includes a cross sections of the  
23 amount of oxygen consumed by the remineralization of organic matter indicating the large  
24 influence of organic matter export in the eastern tropical Pacific OMZ as opposed to eastern  
25 South Atlantic OMZ.

26 In the carbon cycle perturbation simulations, the LOZ that currently exists in the western  
27 tropical Pacific meets the criteria of a permanent non-seasonal OMZ for the approximately 3  
28 X CO<sub>2</sub> simulation; however, in <2000 yrs a much stronger OMZ core develops in the 4 X  
29 CO<sub>2</sub> simulation (Fig. 8). The formation occurs northwest of the Gulf of Carpentaria and  
30 expands into the Banda Sea and south along the west coast of Australia. The western tropical  
31 Pacific OMZ forms in the warm water masses of the Indonesian throughflow (ITF), which  
32 brings warm water westward from the Pacific into the Indian Ocean. The OMZ is then

Formatted: Not Highlight

Formatted: Not Highlight

1 expanded by the oxygen-depleted water masses originating from the Leeuwin Current, which  
2 flows south around the west coast of Australia. ~~The controlling mechanism of the formation~~  
3 ~~of the new OMZ core in the model is similar to that of the Indian Ocean OMZ expansion.~~  
4 There is a net loss of export production of POC and a slight increase in DOC in the area  
5 suggesting the main control of OMZ core formation in the model is similar to that of the  
6 Indian and Atlantic Ocean OMZ expansion. is loss of O<sub>2</sub> solubility due to increased sea  
7 surface temperature (SST) in an area of This region is an area of high heat transport between  
8 the Pacific and Indian Oceans. The formation of an OMZ could be expected in this area of  
9 higher SST; however, it is important to note that the model simulation does not include  
10 changes in the intense tidal induced mixing that may affect sea surface temperatures and  
11 dissolved oxygen concentrations within the Indonesian throughflow nor any global changes to  
12 ocean ventilation. Furthermore, the DO concentration in the OMZ core of the western tropical  
13 Pacific Ocean is increased by 15 μmol kg<sup>-1</sup> O<sub>2</sub> with a 50% reduction in ventilation and  
14 therefore the OMZ simulated would not reach the OMZ criteria proposed here at 4 X CO<sub>2</sub> and  
15 a 50% reduction in ventilation.

## 17 6 Conclusions

18 Increased sea surface temperature as a result of CO<sub>2</sub> radiative forcing will likely cause  
19 expansion of present-day tropical OMZs as well as the possibility of the formation of new  
20 oxygen depleted regions. Understanding the extent and the mechanisms for these OMZ  
21 expansions and how models respond to changes in expansion mechanism is of the utmost  
22 importance in order to more accurately predict environmental changes in these regions.  
23 Simulated expansion of the oxygen minimum zones in this model study is-are greatest in the  
24 eastern tropical Pacific Ocean, which is indicating that the model is more sensitivity to the  
25 change in export of particulate organic carbon which is overestimated by the model, and less  
26 sensitive to loss of surface oxygen solubility in the tropical Pacific Ocean. Total production  
27 increases most in the equatorial Pacific leading to the rapid horizontal expansion of the OMZ  
28 core. Total production is overestimated by the model in the tropical Pacific  
29 Ocean. Furthermore, However, a change in the ecosystem structure could alter the C:N  
30 stoichiometry (carbon overconsumption) and therefore the expansion of the OMZ in the  
31 eastern equatorial Pacific Ocean could be reduced due to decrease in the export production of  
32 POC.

Formatted: Highlight

1 A rise in ~~the seawater temperature and high salinity~~  $P_{POC}$  (2 X and 4 X  $CO_2$  simulations) and  
2 ~~dissolved organic carbon (6 X and 8 X  $CO_2$  simulations)~~ in conjunction with changes in  
3 ~~solubility in the Atlantic Ocean surface water~~ leads to the greatest loss of ~~simulated~~ dissolved  
4 oxygen in the intermediate water masses of any of the OMZs. ~~simulated~~ ~~Dissolved~~  
5 ~~oxygen~~ This loss ~~in solubility~~ causes a greater shoaling and deepening in the eastern tropical  
6 South Atlantic OMZ ~~in the model~~ rather than horizontal expansion. The Indian Ocean OMZ is  
7 restricted in horizontal expansion; therefore, simulated changes in this OMZ are mostly a  
8 vertical expansion of the core, which expands at a similar rate as the eastern tropical South  
9 Atlantic OMZ. ~~This simulated expansion is due to loss of oxygen solubility~~ ~~loss of solubility~~  
10 ~~and an increase in oxygen available for remineralization due to increased concentration of~~  
11 ~~dissolved organic carbon in the a region~~, which is already at very low ~~dissolved~~ oxygen  
12 concentrations.

13 In conclusion, as sea surface temperature increases as a result of  $CO_2$  emission the OMZs will  
14 expand and strengthen as a result of changes ~~in solubility and~~ ~~in~~ export of  $POC$ ,  $DO$ ,  
15 ~~solubility and ventilation~~. These changes will limit migration and habitat zones resulting in  
16 fundamental changes in the marine ecosystem. The loss of dissolved oxygen will also result in  
17 changes to the carbon and nitrogen cycles. Any expansion of hypoxia into the photic zone  
18 could be detrimental to marine ecosystems. Further research on the expansion of OMZ should  
19 include changes in ocean circulation ~~due to changes in density~~ and increased stratification in a  
20 comprehensive earth system model (see e.g. Moore et al. 2013). Changes in the ventilation of  
21 the ocean waters could lead to changes in both the intensity of the oxygen minimum zones as  
22 well as any future expansion.

## 24 Acknowledgements

25 We acknowledge all those who have worked on and with the HAMOCC model, most notably  
26 the late Dr. Ernst Maier-Reimer and Dr. Virginia Palastanga. Plotting was accomplished on  
27 NCAR computers, which are supported by the National Science Foundation. This research is  
28 supported by NSF grants EAR-0628336 and OCE-1536630 as well as NSF STEM support  
29 and UTA graduate dissertation fellowship.

## 1 **References**

- 2 Arakawa, A. and Lamb, V.: Computational design of the basic dynamical processes of the UCLA  
3 General Circulation Model, *Methods in Computational Physics*, 17, 174-267, 1977.
- 4 Archer, D.: Fate of fossil fuel CO<sub>2</sub> in geologic time, *Journal of Geophysical Research: Oceans* (1978–  
5 2012), 110, 2005.
- 6 Archer, D., Eby, M., Brovkin, V., Ridgwell, A., Cao, L., Mikolajewicz, U., Caldeira, K., Matsumoto,  
7 K., Munhoven, G. and Montenegro, A.: Atmospheric lifetime of fossil fuel carbon dioxide, *Annu.*  
8 *Rev. Earth Planet. Sci.*, 37, 117, 2009.
- 9 Beaty-Sykes, T. M.: Effects of climate change and perturbation in biogeochemical cycles on oxygen  
10 distribution and ocean acidification, PhD Dissertation, University of Texas, Arlington, 2014.
- 11 Bopp, L., Le Quéré, C., Heimann, M., Manning, A. C. and Monfray, P.: Climate-induced oceanic  
12 oxygen fluxes: Implications for the contemporary carbon budget, *Global Biogeochem. Cycles*, 16,  
13 1022, 2002.
- 14 Bopp, L., Resplandy, L., Orr, J. C., Doney, S. C., Dunne, J. P., Gehlen, M., Halloran, P., Heinze, C.,  
15 Ilyina, T. and Séférian, R.: Multiple stressors of ocean ecosystems in the 21st century: projections  
16 with CMIP5 models., *Biogeosciences Discussions*, 10, 2013.
- 17 Caldeira, K. and Wickett, M. E.: Oceanography: anthropogenic carbon and ocean pH, *Nature*, 425,  
18 365-365, 2003.
- 19 Cannariato, K. G. and Kennett, J. P.: Climatically related millennial-scale fluctuations in strength of  
20 California margin oxygen-minimum zone during the past 60 ky, *Geology*, 27, 975-978, 1999.
- 21 Deutsch, C., Sarmiento, J. L., Sigman, D. M., Gruber, N. and Dunne, J. P.: Spatial coupling of  
22 nitrogen inputs and losses in the ocean, *Nature*, 445, 163-167, 2007.
- 23 Dunne, J. P., Armstrong, R. A., Gnanadesikan, A. and Sarmiento, J. L.: Empirical and mechanistic  
24 models for the particle export ratio, *Global Biogeochem. Cycles*, 19, 2005.
- 25 Falkowski, P. G., Knoll, A. H., Falkowski, P. and Knoll, A.: An introduction to primary producers in  
26 the sea: who they are, what they do, and when they evolved, *Evolution of Primary Producers in the*  
27 *Sea*, 1-6, 2007.

1 Falkowski, P., Algeo, T., Codispoti, L., Deutsch, C., Emerson, S., Hales, B., Huey, R., LyONS, T.,  
2 NELSON, N. and SCHOFIELD, O.: Ocean De oxygen ation: Past, Present, and Future, *Eos*, 92, 2011.

3 Fuenzalida, R., Schneider, W., Garcés-Vargas, J., Bravo, L. and Lange, C.: Vertical and horizontal  
4 extension of the oxygen minimum zone in the eastern South Pacific Ocean, *Deep Sea Research Part II:*  
5 *Topical Studies in Oceanography*, 56, 992-1003, 2009.

6 Galbraith, E. D., Kienast, M., Pedersen, T. F. and Calvert, S. E.: Glacial-interglacial modulation of the  
7 marine nitrogen cycle by high-latitude O<sub>2</sub> supply to the global thermocline, *Paleoceanography*, 19,  
8 2004.

9 Garcia, H. E., Boyer, T. P., Locarnini, R. A., Antonov, J. I., Mishonov, A. V., Baranova, O. K.,  
10 Zweng, M. M., Reagan, J. R., Johnson, D. R. and Levitus, S.: *World Ocean Atlas 2013: Dissolved*  
11 *Oxygen, Apparent Oxygen Utilization, and Oxygen Saturation*, 2013.

12 Glessmer, M., Park, W. and Oschlies, A.: Simulated reduction in upwelling of tropical oxygen  
13 minimum waters in a warmer climate, *Environmental Research Letters*, 6, 045001, 2011.

14 Gray, J. S., Wu, R. S. and Or, Y. Y.: Effects of hypoxia and organic enrichment on the coastal marine  
15 environment, *Mar. Ecol. Prog. Ser.*, 238, 249-279, 2002.

16 Hansen, J., Fung, I., Lacis, A., Rind, D., Lebedeff, S., Ruedy, R., Russell, G. and Stone, P.: Global  
17 climate changes as forecast by Goddard Institute for Space Studies three-dimensional model, *Journal*  
18 *of Geophysical Research: Atmospheres* (1984–2012), 93, 9341-9364, 1988.

19 Heinze, C.: Simulating oceanic CaCO<sub>3</sub> export production in the greenhouse, *Geophys. Res. Lett.*, 31,  
20 2004.

21 Heinze, C., Kriest, I., and Maier-Reimer, E.: Age offsets among different biogenic and lithogenic  
22 components of sediment cores revealed by numerical modeling, *Paleoceanography*, 24.4, 2009.  
23 Doi:10.1029/2008PA001662

24 Heinze, C., Gehlen, M. and Land, C.: On the potential of <sup>230</sup>Th, <sup>231</sup>Pa, and <sup>10</sup>Be for marine rain  
25 ratio determinations: A modeling study, *Global Biogeochem. Cycles*, 20, 2006.

26 Heinze, C. and Maier-Reimer, E.: The hamburg oceanic carbon cycle circulation model version  
27 “HAMOCC2s” for long time integrations, DKRZ, 1999.

- 1 Heinze, C., Maier-Reimer, E., Winguth, A. M. and Archer, D.: A global oceanic sediment model for  
2 long-term climate studies, *Global Biogeochem. Cycles*, 13, 221-250, 1999.
- 3 Heinze, C., Maier-Reimer, E. and Winn, K.: Glacial pCO<sub>2</sub> reduction by the world ocean: Experiments  
4 with the Hamburg carbon cycle model, *Paleoceanography*, 6, 395-430, 1991.
- 5 Helly, J. J. and Levin, L. A.: Global distribution of naturally occurring marine hypoxia on continental  
6 margins, *Deep Sea Research Part I: Oceanographic Research Papers*, 51, 1159-1168, 2004.
- 7 IPCC 2013.: The IPCC Fifth Assessment Report (AR5), *Climate Change 2013: The Physical Science*  
8 *Basis*. Intergovernmental Panel on Climate Change, Geneva, Switzerland, 2014.
- 9 John Theodore Houghton: *Global Warming*, Cambridge University Press, 2004.
- 10 Kamykowski, D. and Zentara, S.: Hypoxia in the world ocean as recorded in the historical data set,  
11 *Deep Sea Research Part A. Oceanographic Research Papers*, 37, 1861-1874, 1990.
- 12 Karl, T. R., Arguez, A., Huang, B., Lawrimore, J. H., McMahon, J. R., Menne, M. J., Peterson, T. C.,  
13 Vose, R. S. and Zhang, H. M.: CLIMATE CHANGE. Possible artifacts of data biases in the recent  
14 global surface warming hiatus, *Science*, 348, 1469-1472, 10.1126/science.aaa5632 [doi], 2015.
- 15 Karstensen, J., Fiedler, B., Schütte F., Brandt, P., Körtzinger, A., Fischer, G., Zantopp, R., Hahn, J.,  
16 Visbeck, M., and Wallace, D.: Open ocean dead zones in the tropical North Atlantic Ocean,  
17 *Biogeosciences Discussions*, 11(12), 17391-17411, 2014.
- 18 Karstensen, J., Stramma, L. and Visbeck, M.: Oxygen minimum zones in the eastern tropical Atlantic  
19 and Pacific oceans, *Prog. Oceanogr.*, 77, 331-350, 2008.
- 20 Keeling, R. F., Körtzinger, A. and Gruber, N.: Ocean deoxygenation in a warming world, *Annual*  
21 *Review of Marine Science*, 2, 199-229, 2010.
- 22 Levitus, S., Antonov, J., Baranova, O., Boyer, T., Coleman, C., Garcia, H., Grodsky, A., Johnson, D.,  
23 Locarnini, R. and Mishonov, A.: The World Ocean Database, *Data Science Journal*, 12, WDS229-  
24 WDS234, 2013.
- 25 Locarnini, R., Mishonov, A., Antonov, J., Boyer, T., Garcia, H., Baranova, O., Zweng, M., Paver, C.,  
26 Reagan, J. and Johnson, D.: *World Ocean Atlas 2013. Vol. 1: Temperature*, A. Mishonov, Technical  
27 Ed. NOAA Atlas NESDIS, 73, 40, 2013.

1 Mahowald, N. M., Muhs, D. R., Levis, S., Rasch, P. J., Yoshioka, M., Zender, C. S. and Luo, C.:  
2 Change in atmospheric mineral aerosols in response to climate: Last glacial period, preindustrial,  
3 modern, and doubled carbon dioxide climates, *Journal of Geophysical Research*, 111, D10202, 2006.

4 Maier-Reimer, E.: Geochemical cycles in an ocean general circulation model. Preindustrial tracer  
5 distributions, *Global Biogeochem. Cycles*, 7, 645-677, 1993.

6 Maier-Reimer, E. and Heinze, C.: , The Hamburg oceanic carbon cycle circulation model.Cycle 1,  
7 1992.

8 Maier-Reimer, E. and Hasselmann, K.: Transport and storage of CO<sub>2</sub> in the ocean—an inorganic  
9 ocean-circulation carbon cycle model, *Clim. Dyn.*, 2, 63-90, 1987.

10 Maier-Reimer, E., Mikolajewicz, U. and Hasselmann, K.: Mean circulation of the Hamburg LSG  
11 OGCM and its sensitivity to the thermohaline surface forcing, *J. Phys. Oceanogr.*, 23, 731-757, 1993.

12 Maier-Reimer, E., Mikolajewicz, U. and Winguth, A.: Future ocean uptake of CO<sub>2</sub>: interaction  
13 between ocean circulation and biology, *Clim. Dyn.*, 12, 711-722, 1996.

14 Matear, R., Hirst, A. and McNeil, B.: Changes in dissolved oxygen in the Southern Ocean with  
15 climate change, *Geochem. Geophys. Geosyst.*, 1, 2000.

16 Moore, J. K., Lindsay, K., Doney, S. C., Long, M. C. and Misumi, K.: Marine Ecosystem Dynamics  
17 and Biogeochemical Cycling in the Community Earth System Model [CESM1 (BGC)]: Comparison of  
18 the 1990s with the 2090s under the RCP4. 5 and RCP8. 5 Scenarios., *J. Clim.*, 26, 2013.

19 Najjar, R. G., Sarmiento, J. L. and Toggweiler, J.: Downward transport and fate of organic matter in  
20 the ocean: Simulations with a general circulation model, *Global Biogeochem. Cycles*, 6, 45-76, 1992.

21 Oschlies, A., Schulz, K. G., Riebesell, U. and Schmittner, A.: Simulated 21st century's increase in  
22 oceanic suboxia by CO<sub>2</sub>-enhanced biotic carbon export, *Global Biogeochem. Cycles*, 22, 2008.

23 Palastanga, V., Slomp, C. and Heinze, C.: Glacial-interglacial variability in ocean oxygen and  
24 phosphorus in a global biogeochemical model, *Biogeosciences*, 10, 945-958, 2013.

25 Palastanga, V., Slomp, C. and Heinze, C.: Long-term controls on ocean phosphorus and oxygen in a  
26 global biogeochemical model, *Global Biogeochem. Cycles*, 25, 2011.

- 1 Parsons, T. and Takahashi, M.: Environmental control of phytoplankton cell size, *Limnol. Oceanogr.*,  
2 18, 511-515, 1973.
- 3 Paulmier, A., Ruiz-Pino, D. and Garçon, V.: CO<sub>2</sub> maximum in the oxygen minimum zone (OMZ),  
4 *Biogeosciences*, 8, 239-252, 2011.
- 5 Riebesell, U., Schulz, K. G., Bellerby, R. G. J., Botros, M., Fritsche, P., Meyerhöfer, M., Neill, C.,  
6 Nondal, G., Oschlies, A., Wohlers, J., and Zöllner, E.: Enhanced biological carbon consumption in a  
7 high CO<sub>2</sub> ocean, *Nature*, 450(7169), 545-548, 2007. doi:10.1038/nature06267
- 8 Ruddiman, W. F.: *Earth's Climate: past and future*, Macmillan, 2001.
- 9 Sarmiento, J. L., Hughes, T. M., Stouffer, R. J. and Manabe, S.: Simulated response of the ocean  
10 carbon cycle to anthropogenic climate warming, *Nature*, 393, 245-249, 1998.
- 11 Sarmiento, J. L. and Orr, J. C.: Three-dimensional simulations of the impact of Southern Ocean  
12 nutrient depletion on atmospheric CO<sub>2</sub> and ocean chemistry, *Limnol. Oceanogr.*, 36, 1928-1950,  
13 1991.
- 14 Sarmiento, J. L. and Gruber, N.: *Ocean biogeochemical dynamics*, Princeton University Press  
15 Princeton, 2006.
- 16 Schmittner, A., Oschlies, A., Matthews, H. D. and Galbraith, E. D.: Future changes in climate, ocean  
17 circulation, ecosystems, and biogeochemical cycling simulated for a business-as-usual CO<sub>2</sub> emission  
18 scenario until year 4000 AD, *Global Biogeochem. Cycles*, 22, GB1013, 2008.
- 19 Shaffer, G., Olsen, S. M. and Pedersen, J. O. P.: Long-term ocean oxygen depletion in response to  
20 carbon dioxide emissions from fossil fuels, *Nature Geoscience*, 2, 105-109, 2009.
- 21 Stramma, L., Oschlies, A. and Schmidtko, S.: Anticorrelated observed and modeled trends in  
22 dissolved oceanic oxygen over the last 50 years, *Biogeosciences Discussions*, 9, 4595-4626, 2012.
- 23 Stramma, L., Visbeck, M., Brandt, P., Tanhua, T., and Wallace, D.: Deoxygenation in the oxygen  
24 minimum zone of the eastern tropical North Atlantic, *Geophysical Research Letters* 36(20), 2009.
- 25 Stramma, L., Johnson, G. C., Sprintall, J. and Mohrholz, V.: Expanding oxygen-minimum zones in the  
26 tropical oceans, *Science*, 320, 655-658, 2008.

- 1 Volk, T. and Hoffert, M. I.: Ocean carbon pumps: Analysis of relative strengths and efficiencies in  
2 ocean-driven atmospheric CO<sub>2</sub> changes, *The Carbon Cycle and Atmospheric CO<sub>2</sub>: Natural Variations*  
3 *Archean to Present*, 99-110, 1985.
- 4 Weiss, R.: The solubility of nitrogen, oxygen and argon in water and seawater, in: *Deep Sea Research*  
5 *and Oceanographic Abstracts*, 1970.
- 6 Whitney, F. A., Freeland, H. J. and Robert, M.: Persistently declining oxygen levels in the interior  
7 waters of the eastern subarctic Pacific, *Prog. Oceanogr.*, 75, 179-199, 2007.
- 8 Winguth, A., Mikolajewicz, U., Gröger, M., Maier-Reimer, E., Schurgers, G. and Vizcaíno, M.:  
9 Centennial-scale interactions between the carbon cycle and anthropogenic climate change using a  
10 dynamic Earth system model, *Geophys. Res. Lett.*, 32, 2005.
- 11 Winguth, A., Archer, D., Duplessy, J., Maier-Reimer, E. and Mikolajewicz, U.: Sensitivity of  
12 paleonutrient tracer distributions and deep-sea circulation to glacial boundary conditions,  
13 *Paleoceanography*, 14, 304-323, 1999.
- 14 Zachos, J. C., Dickens, G. R. and Zeebe, R. E.: An early Cenozoic perspective on greenhouse warming  
15 and carbon-cycle dynamics, *Nature*, 451, 279-283, 2008.
- 16 Zweng, M., Reagan, J., Antonov, J., Locarnini, R., Mishonov, A., Boyer, T., Garcia, H., Baranova, O.,  
17 Johnson, D. and Seidov, D.: *World Ocean Atlas 2013. Vol. 2: Salinity*, NOAA Atlas NESDIS, 74, 39,  
18 2013.
- 19

1 Table 1. List of initial conditions.

2 Table 2. List of model scenarios.

3 Figure 1. Atmospheric pCO<sub>2</sub> and sea surface temperature increase from the reference run (a) 2  
4 X CO<sub>2</sub> (b) 4 X CO<sub>2</sub> (c) 6 X CO<sub>2</sub> (d) 8 X CO<sub>2</sub> for the first 500 years of a 30k year simulation.  
5 The red dashed line indicates the preindustrial pCO<sub>2</sub> level.

Formatted: Normal, Left

6 Figure 2. The difference in particulate organic carbon ( $\mu\text{mol kg}^{-1}$ ) for (a) 4 X CO<sub>2</sub> and the  
7 reference simulation, (b) 6 X CO<sub>2</sub> and the reference simulation and (c) 8 X CO<sub>2</sub> simulation  
8 and the reference simulation.

9

10 Figure 23. Locations of the OMZ at 450 meters depth simulated by HAMOCC 2.0 (reference  
11 experiment) [1] Eastern North Pacific OMZ [2] Eastern South Pacific OMZ [3] Eastern South  
12 Atlantic OMZ [4] Indian Ocean.

Formatted: Line spacing: 1.5 lines

13 ~~Figure 6. (a) Dissolved oxygen concentration for the extinction simulations and (b) reference~~  
14 ~~simulation oxygen concentration.~~ Figure 4. Reduced ventilation simulations at (a) reference  
15 (100% ventilation), (b) 25% reduction, (c) 50% reduction, (d) 75% reduction and (e) 100%  
16 reduction in ventilation.

17

Formatted: Normal, Left

18 Figure 53. Dissolved O<sub>2</sub> concentration simulated by (a) the 4 X CO<sub>2</sub> experiment without CO<sub>2</sub>  
19 radiative forcing minus the reference experiment (b) the 4 X CO<sub>2</sub> with CO<sub>2</sub> radiative forcing  
20 simulation minus reference experiment.

21 Figure 6. The horizontal expansion of OMZs at 450 meters depth for the Pacific, Atlantic and  
22 Indian Oceans in the (a) 2 X CO<sub>2</sub> simulation, (b) 4 X CO<sub>2</sub> simulation, (c) 6 X CO<sub>2</sub> simulation  
23 and 8 X CO<sub>2</sub> simulation.

Formatted: Subscript

Formatted: Subscript

Formatted: Subscript

Formatted: Subscript

24

25 Figure 74. Simulated vertical distribution of dissolved O<sub>2</sub> through the OMZ cores for a)  
26 Eastern North Pacific OMZ [110°W, 10°N], b) Eastern South Pacific OMZ [85°W, 10°S], c)  
27 Eastern South Atlantic OMZ [5°W, 10°S], and d) Indian Ocean OMZ [Gulf of Bengal; 85°E,  
28 7°N] for the 1 X, 4 X and 8 X CO<sub>2</sub> simulations (top). The bottom row are finer scale  
29 dissolved oxygen profiles for the OMZ cores e) Eastern North Pacific OMZ, f) Eastern South  
30 Pacific OMZ, g) Eastern South Atlantic OMZ, and h) Indian Ocean OMZ for the 1 X, 4 X and

1 8 X CO<sub>2</sub> simulations. Observations are the annual statistical mean for dissolved oxygen from  
2 the World Ocean Atlas, 2013 (Garcia et al., 2014). Standard error of the mean; upper ocean:  
3 0.54-2.86 μmol L<sup>-1</sup>, twilight zone: 0.42-2.32 μmol L<sup>-1</sup>, deep ocean: 0.36-1.98 μmol L<sup>-1</sup>.

4 Figure 5. Zonal cross-section at 1.25° N of the formation of the western tropical Pacific OMZ  
5 for the (a) 2 X, (b) 4 X and (c) 8 X CO<sub>2</sub> simulations. The OMZ core is located between 130°E  
6 and 150°E.

7 Figure 7. (a) Difference in export production of POC between the 8 X CO<sub>2</sub> experiment and  
8 reference experiment, (b) dissolved oxygen at 450 m depth for the 8 X CO<sub>2</sub> experiment, (c)  
9 difference in air-sea gas exchange between the 8 X CO<sub>2</sub> experiment and the reference  
10 experiment, and (d) sea-water temperature at 450 m depth. The numbers indicate the OMZ  
11 locations; [1] Eastern tropical North Pacific; 110°W, 10°N. [2] eastern tropical South Pacific;  
12 85°W, 10°S. [3] eastern tropical South Atlantic; 5°W, 10°S. [4] Indian Ocean (Gulf of  
13 Bengal); 85°E, 7°N.

14 Figure 8. (a) Lost due to remineralization of particulate organic carbon for the reference run  
15 [μmol m<sup>-2</sup> yr<sup>-1</sup>]. Difference between the loss of oxygen due to remineralization between (b) 2  
16 X CO<sub>2</sub> and reference run, (c) 4 X CO<sub>2</sub> and reference run (d) 8 X CO<sub>2</sub> and reference  
17 experiment. Figure 8. Zonal cross-section at 1.25° N of the formation of the western tropical  
18 Pacific OMZ for the (a) 2 X, (b) 4 X and (c) 8 X CO<sub>2</sub> simulations. The OMZ core is located  
19 between 130° E and 150°E.

20 Figure 9. The difference in the dissolved oxygen concentration between (a) the 50% reduction  
21 in ventilation and the 4 X CO<sub>2</sub> simulation with radiative forcing and (b) the 75% reduction in  
22 ventilation and the 4 X CO<sub>2</sub> simulation with radiative forcing.

23 Figure 10. Mechanisms for oxygen loss in the OMZs at 8 X CO<sub>2</sub>. (a) Reference simulation.  
24 (b) The difference in DO concentrations between 8 X CO<sub>2</sub> and the reference simulation. (c)  
25 The difference in DO lost due to changes in solubility between 8 X CO<sub>2</sub> and the reference  
26 simulation. (d) The increase in oxygen consumption due to remineralization of organic carbon  
27 between the 8 X CO<sub>2</sub> and reference simulation.

28 Figure 11. Mechanisms for oxygen loss in the OMZs at 4 X CO<sub>2</sub>. (a) Reference simulation.  
29 (b) The difference in DO concentrations between 8 X CO<sub>2</sub> and the reference simulation. (c)  
30 The difference in DO lost due to changes in solubility between 8 X CO<sub>2</sub> and the reference

Formatted: Subscript

1 simulation. (d) The increase in oxygen consumption due to remineralization of organic carbon  
2 between the 4 X CO<sub>2</sub> and reference simulation.

Formatted: Subscript

3

4

Formatted: Normal, Left

5

6

7

1 Table 1. List of initial conditions.

Water Column		Atmosphere	
Parameter	Value (mol L <sup>-1</sup> )	Parameter	Value (ppmv)
<a href="#">sCO<sub>2</sub>DIC</a> <sup>12</sup>	2.25 E <sup>-3</sup>	CO <sub>2</sub>	279.78
Alkalinity	2.33 (eq)	O <sub>2</sub>	209761
PO <sub>4</sub>	2.54 E <sup>-4</sup>		
O <sub>2</sub>	1.65 E <sup>-4</sup>		
Fe dust	6.0 E <sup>-10</sup>		

Formatted Table

Formatted: Superscript

Table 2. List of model scenarios.

Increased pCO <sub>2</sub> without Radiative Forcing	Increased pCO <sub>2</sub> with Radiative Forcing	Atmospheric CO <sub>2</sub> Concentration (ppmv)	Integration Time (years)	Brief Description of the Simulation
<b>CO<sub>2</sub> Stabilization Simulations</b>				
1 X CO <sub>2</sub>		279.78	30,000	Reference simulation with preindustrial atmospheric CO <sub>2</sub> levels.
2 X CO <sub>2</sub> _nf	2 X CO <sub>2</sub> _f	559.56	30,000	Experiments with no feedbacks (nf) have an increase of pCO <sub>2</sub> of 1% per year without temperature feedbacks. Temperature changes are applied in experiments with feedbacks (f) as a function of pCO <sub>2</sub> after Hansen et al. (1988) resulting in a seawater temperature change of 2.8°C, 5.9°C, 8.7°C and 11.5°C for 2 X, 4 X, 6 X and 8 X CO <sub>2</sub> , respectively.
3 X CO <sub>2</sub> _nf	3 X CO <sub>2</sub> _f	839.34	30,000	
4 X CO <sub>2</sub> _nf	4 X CO <sub>2</sub> _f	1,119.12	30,000	
6 X CO <sub>2</sub> _nf	6 X CO <sub>2</sub> _f	1,678.68	30,000	
8 X CO <sub>2</sub> _nf	8 X CO <sub>2</sub> _f	2,238.24	30,000	
<b>Kill-Biology Simulations</b>				
Kill_All_Prod		279.78	1000	Kill_All_Prod is simulated as an extinction simulation with primary productivity (POC, Si, CaCO <sub>3</sub> ) reduced to 1X10 <sup>-20</sup> PgC yr <sup>-1</sup> and present day atmospheric O <sub>2</sub> concentrations.
<b>Preindustrial P<sub>POC</sub> with Increasing Atmospheric pCO<sub>2</sub> Simulations</b>				
	2 X CO <sub>2</sub> _POC	559.56	10,000	Experiments for static POC with changing atmospheric pCO <sub>2</sub> concentrations involve prescribing POC to a preindustrial value that does not evolve with model integration.
	4 X CO <sub>2</sub> _POC	1,119.12	10,000	
	8 X CO <sub>2</sub> _POC	2,238.24	10,000	
<b>Reduced Ventilation Simulations</b>				
Vent_25		279.78	10,000	Experiments with reduction in ventilation include a simulation in which ventilation (vertical, horizontal and meridional) is reduced by 25%, 50%, 75% and 100%. Atmospheric pCO <sub>2</sub> remains at preindustrial concentrations for all experiments.

Formatted: Left: 1", Right: 1", Top: 1.25", Bottom: 1.25", Width: 11", Height: 8.5"

Formatted: Font: Times New Roman, 12 pt

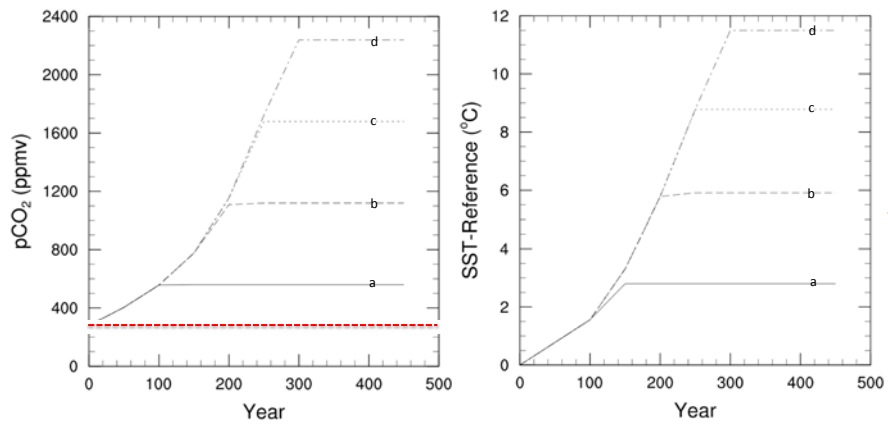


Figure 1. Atmospheric pCO<sub>2</sub> and sea surface temperature increase from the reference run (a) 2 X CO<sub>2</sub> (b) 4 X CO<sub>2</sub> (c) 6 X CO<sub>2</sub> (d) 8 X CO<sub>2</sub> for the first 500 years of a 30k year simulation. The red dashed line indicates the preindustrial pCO<sub>2</sub> level.

Formatted: Section start: New page

Formatted: Normal (Web)

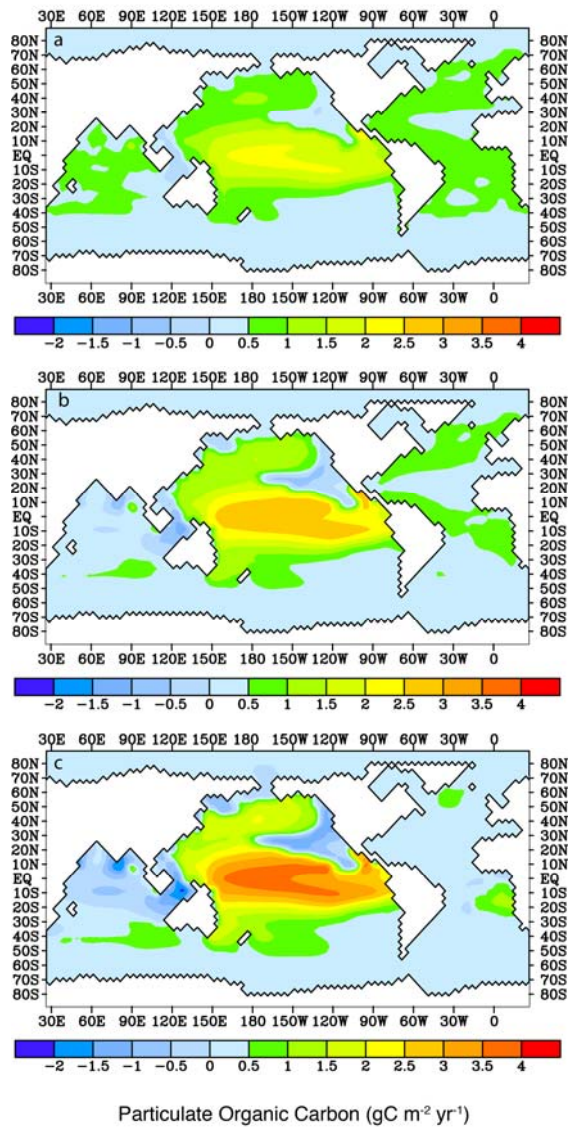


Figure 2. The difference in particulate organic carbon ( $\mu\text{mol kg}^{-1}$ ) for (a) 4 X CO<sub>2</sub> and the reference simulation, (b) 6 X CO<sub>2</sub> and the reference simulation and (c) 8 X CO<sub>2</sub> simulation and the reference simulation.

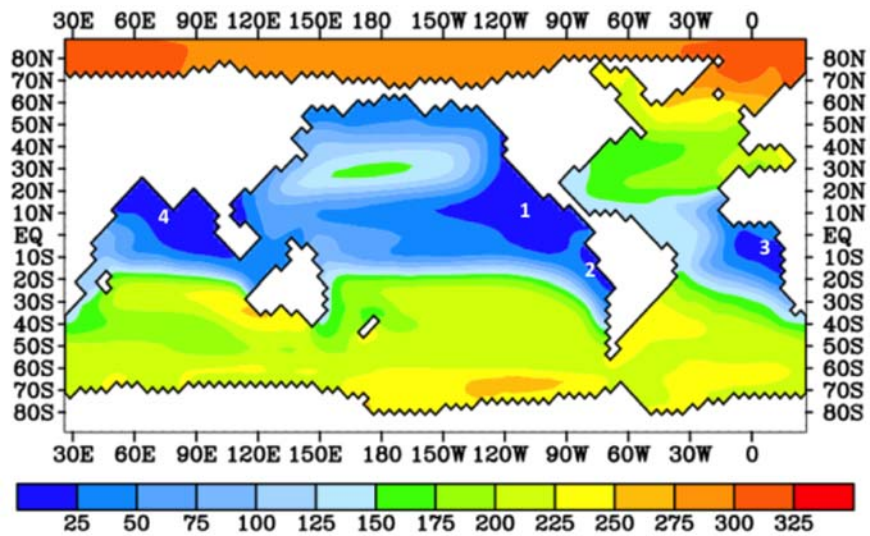
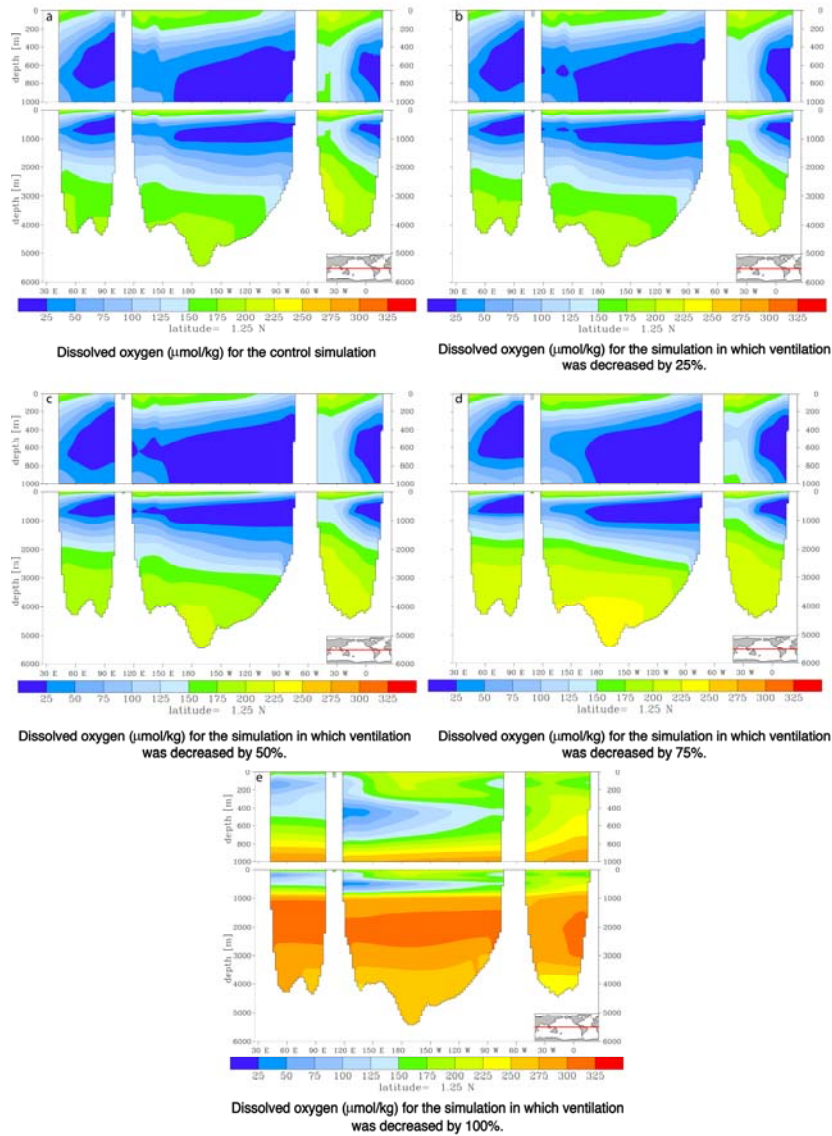


Figure 23. Locations of the OMZ at 450 meters depth simulated by HAMOCC 2.0 (reference experiment) [1] Eastern North Pacific OMZ [2] Eastern South Pacific OMZ [3] Eastern South Atlantic OMZ [4] Indian Ocean.



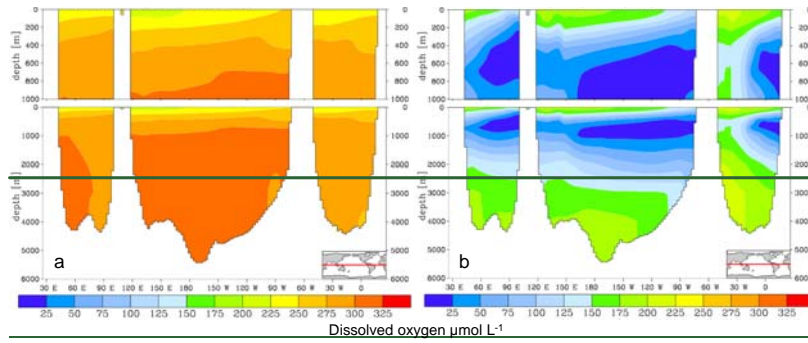


Figure 6. (a) Dissolved oxygen concentration for the extinction simulations and (b) reference simulation oxygen concentration.

Figure 4. Reduced ventilation simulations at (a) reference (100% ventilation), (b) 25% reduction, (c) 50% reduction, (d) 75% reduction and (e) 100% reduction in ventilation.

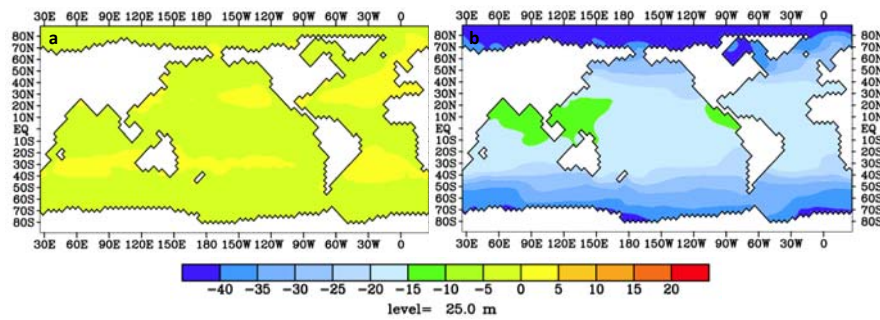


Figure 35. Dissolved O<sub>2</sub> concentration simulated by (a) the 4 X CO<sub>2</sub> experiment without CO<sub>2</sub> radiative forcing minus the reference experiment (b) the 4 X CO<sub>2</sub> with CO<sub>2</sub> radiative forcing simulation minus reference experiment.

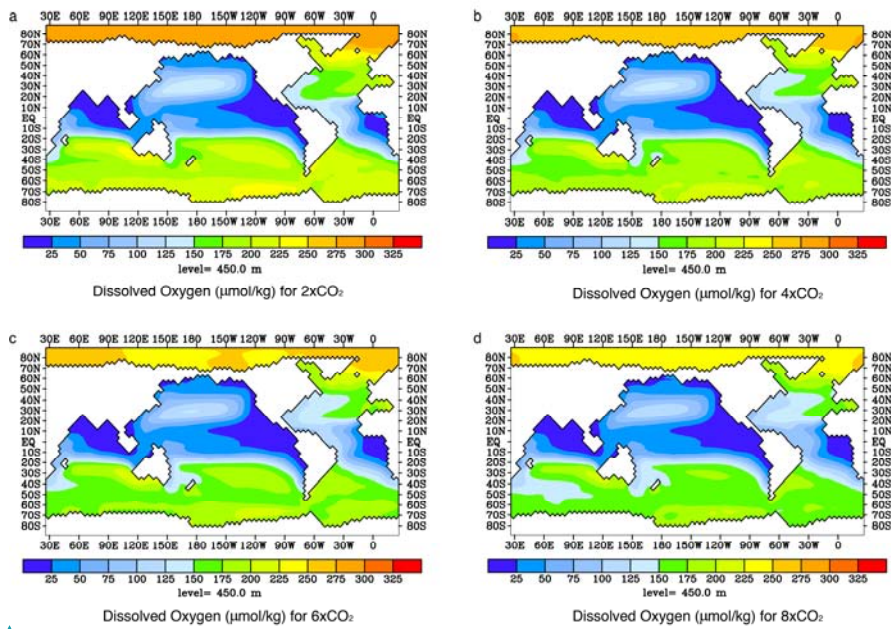


Figure 6. The horizontal expansion of OMZs at 450 meters depth for the Pacific, Atlantic and Indian Oceans in the (a) 2 X CO<sub>2</sub> simulation, (b) 4 X CO<sub>2</sub> simulation, (c) 6 X CO<sub>2</sub> simulation and 8 X CO<sub>2</sub> simulation.

Formatted: Font: Times New Roman, 12 pt

Commented [TS2]: Figure added at the request of reviewer 1. Addition plots will be in supplementary data

Formatted: Normal, Left

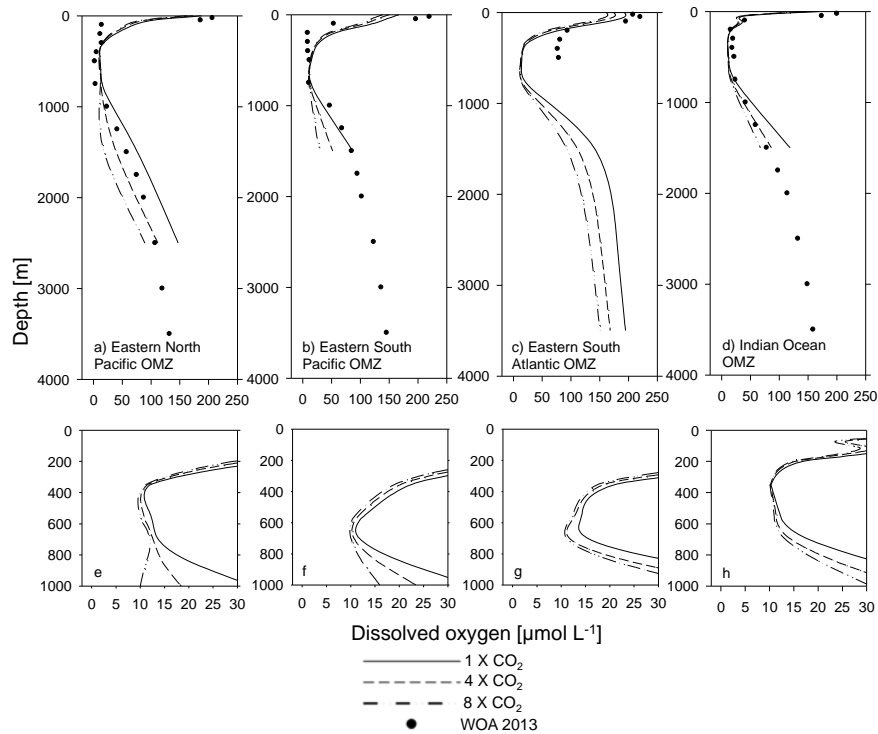
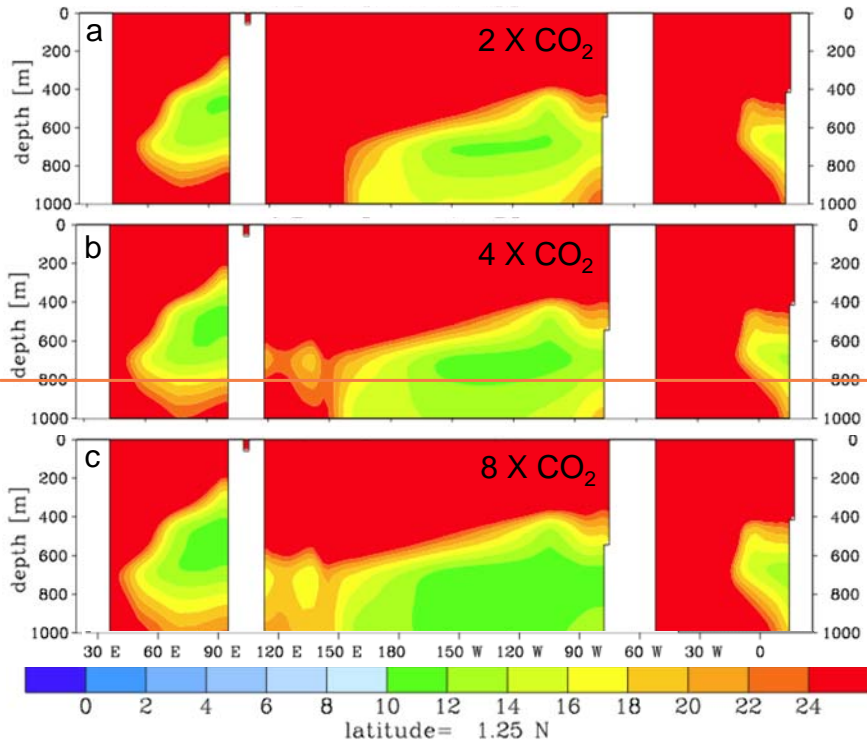


Figure 47. Simulated vertical distribution of dissolved O<sub>2</sub> through the OMZ cores for a) Eastern North Pacific OMZ [110°W, 10°N], b) Eastern South Pacific OMZ [85°W, 10°S], c) Eastern South Atlantic OMZ [5°W, 10°S], and d) Indian Ocean OMZ [Gulf of Bengal; 85°E, 7°N] for the 1 X, 4 X and 8 X CO<sub>2</sub> simulations (top). The bottom row are finer scale dissolved oxygen profiles for the OMZ cores e) Eastern North Pacific OMZ, f) Eastern South Pacific OMZ, g) Eastern South Atlantic OMZ, and h) Indian Ocean OMZ for the 1 X, 4 X and 8 X CO<sub>2</sub> simulations. Observations are the annual statistical mean for dissolved oxygen from the World Ocean Atlas, 2013 (Garcia et al., 2014). Standard error of the mean; upper ocean: 0.54-2.86 μmol L<sup>-1</sup>, twilight zone: 0.42-2.32 μmol L<sup>-1</sup>, deep ocean: 0.36-1.98 μmol L<sup>-1</sup>.





Formatted: Font: Times New Roman, 12 pt

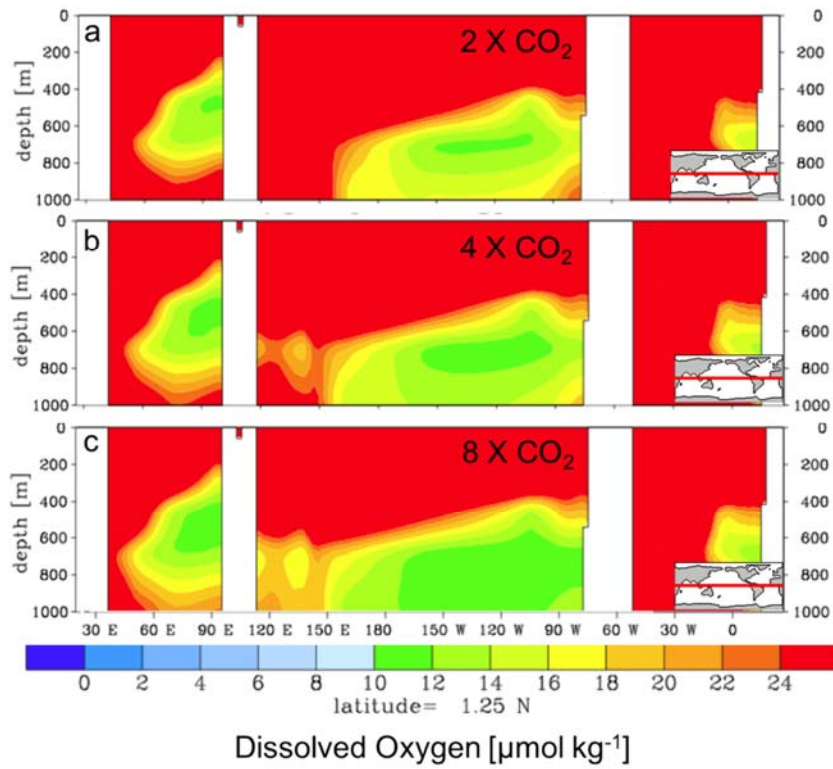


Figure 58. Zonal cross-section at  $1.25^\circ \text{N}$  of the formation of the western tropical Pacific OMZ for the (a) 2 X, (b) 4 X and (c) 8 X  $\text{CO}_2$  simulations. The OMZ core is located between  $130^\circ\text{E}$  and  $150^\circ\text{E}$ .

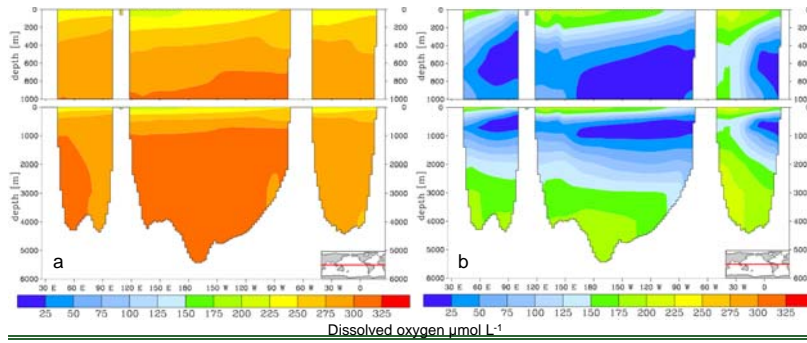


Figure 6. (a) Dissolved oxygen concentration for the extinction simulations and (b) reference simulation oxygen concentration.

Formatted: Caption, Justified

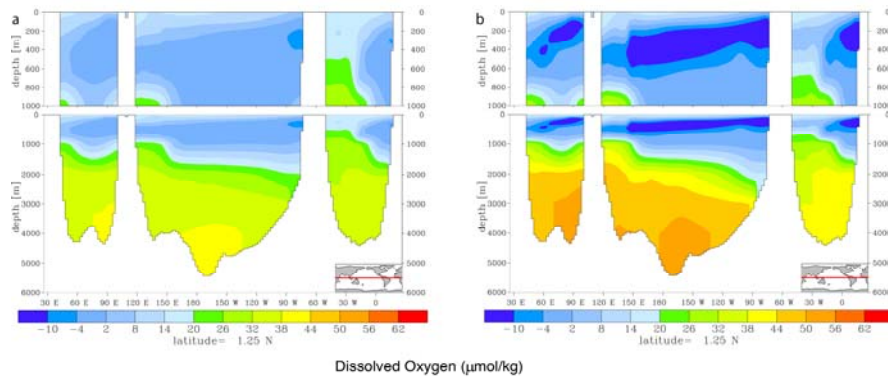


Figure 9. The difference in the dissolved oxygen concentration between (a) the 25% reduction in ventilation and the 4 X CO<sub>2</sub> simulation with radiative forcing and (b) the 50% reduction in ventilation and the 4 X CO<sub>2</sub> simulation with radiative forcing.

Formatted: Font: Times New Roman, 12 pt

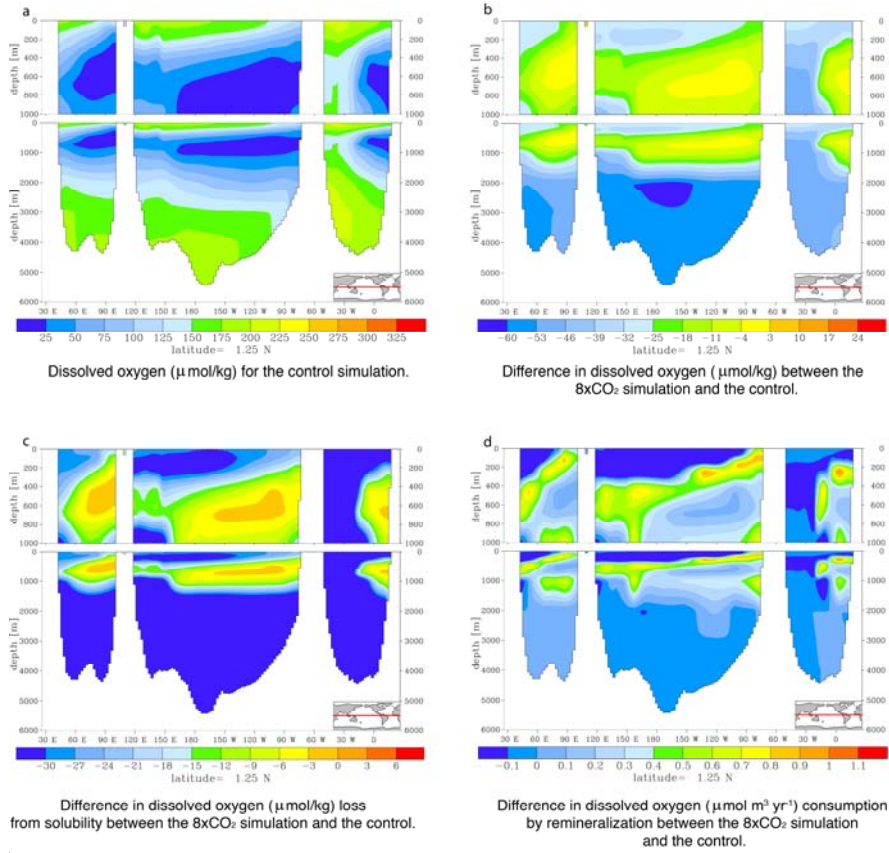
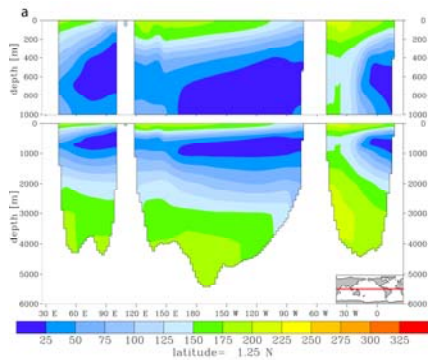


Figure 10. Mechanisms for oxygen loss in the OMZs at 8 X  $\text{CO}_2$ . (a) Reference simulation. (b) The difference in DO concentrations between 8 X  $\text{CO}_2$  and the reference simulation. (c) The difference in DO lost due to changes in solubility between 8 X  $\text{CO}_2$  and the reference simulation. (d) The increase in oxygen consumption due to remineralization of organic carbon between the 8 X  $\text{CO}_2$  and reference simulation.

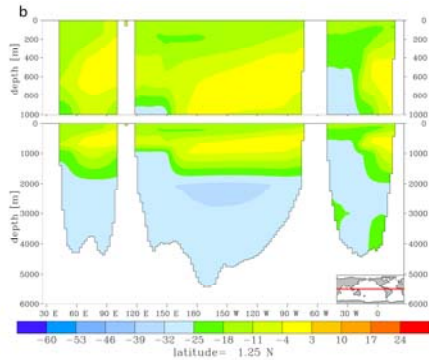
Formatted: English (United States)

Formatted: Normal, Left

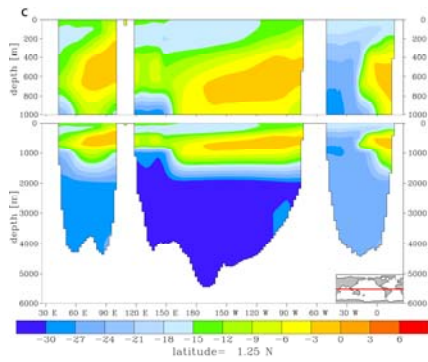
Formatted: Normal, Left



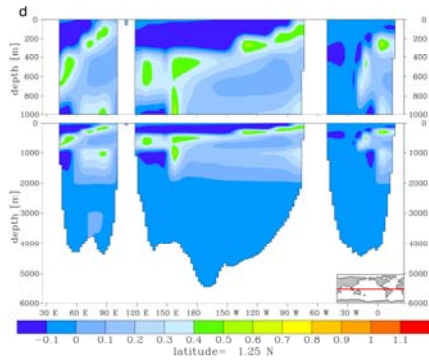
Dissolved oxygen ( $\mu\text{mol/kg}$ ) for the control simulation.



Difference in dissolved oxygen ( $\mu\text{mol/kg}$ ) between the  $4\times\text{CO}_2$  simulation and the control.



Difference in dissolved oxygen ( $\mu\text{mol/kg}$ ) loss from solubility between the  $4\times\text{CO}_2$  simulation and the control.



Difference in dissolved oxygen ( $\mu\text{mol m}^3 \text{yr}^{-1}$ ) consumption by remineralization between the  $4\times\text{CO}_2$  simulation and the control.

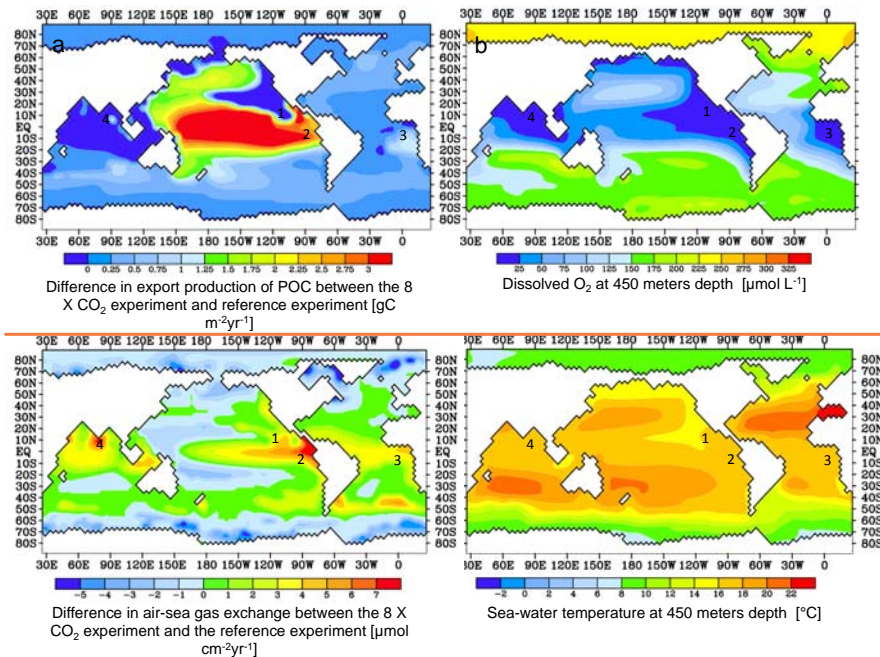


Figure 7. (a) Difference in export production of POC between the 8 X CO<sub>2</sub> experiment and reference experiment, (b) dissolved oxygen at 450 m depth for the 8 X CO<sub>2</sub> experiment, (c) difference in air sea gas exchange between the 8 X CO<sub>2</sub> experiment and the reference experiment, and (d) sea water temperature at 450 m depth. The numbers indicate the OMZ locations; [1] Eastern tropical North Pacific; 110°W, 10°N. [2] eastern tropical South Pacific; 85°W, 10°S. [3] eastern tropical South Atlantic; 5°W, 10°S. [4] Indian Ocean (Gulf of Bengal); 85°E, 7°N.

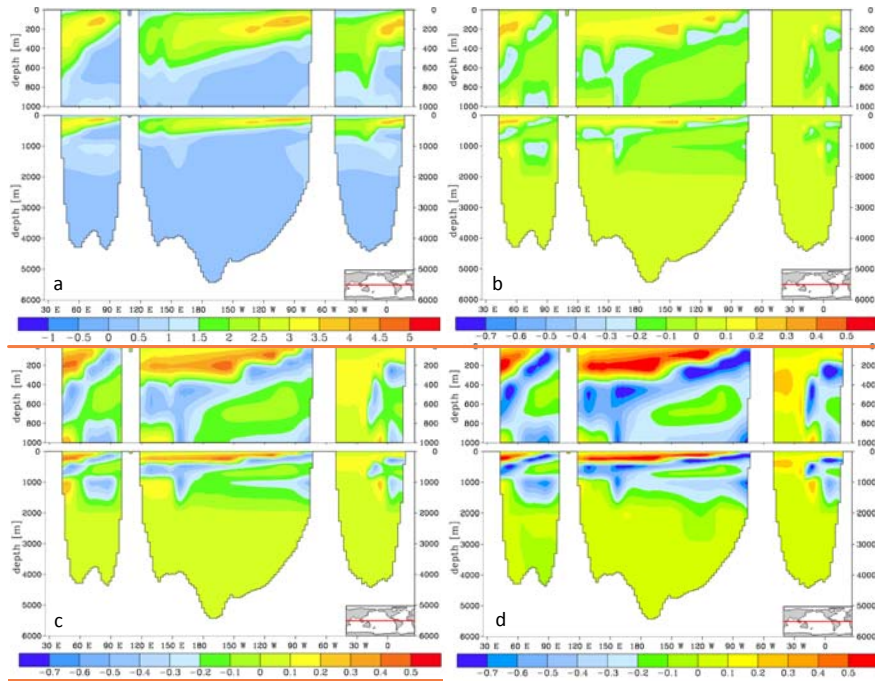


Figure 11. Mechanisms for oxygen loss in the OMZs at 4 X CO<sub>2</sub>. (a) Reference simulation. (b) The difference in DO concentrations between 4 X CO<sub>2</sub> and the reference simulation. (c) The difference in DO lost due to changes in solubility between 4 X CO<sub>2</sub> and the reference simulation. (d) The increase in oxygen consumption due to remineralization of organic carbon between the 4 X CO<sub>2</sub> and reference simulation.

Figure 8. (a) Lost due to remineralization of particulate organic carbon for the reference run [ $\mu\text{mol} \cdot \text{m}^{-2} \cdot \text{yr}^{-1}$ ]. Difference between the loss of oxygen due to remineralization between (b) 2 X CO<sub>2</sub> and reference run, (c) 4 X CO<sub>2</sub> and reference run (d) 8 X CO<sub>2</sub> and reference experiment.